TABLE IV The difference of TAP phenotype frequency among different ethnics

	Behçet's disease		Controls		
	Japanese ($n = 46$) (%)	Spanish*($n = 58$) (%)	Japanese ($n = 95$) (%)	Spanish*($n = 116$) (%)	UK†($n = 58$) (%)
TAP1					
A	100	100	96.8	93.9	99.3
B	21.7	24.1	26.3	26.7	15.0
C	4.3	0.0	0.0	12.1	1.8
TAP2					
A	65.2	83.8	65.3	78.5	81.4
B	54.3	50.0	60.0	57.8	54.8
C	23.9	22.4	23.2	24.1	10.1

UK:United Kingdom
* Gonza'lez-Escribano *et al.*[11]
† Wordsworth *et al.*[24]

In this study, no significant differences were observed between patients with BD and control population in the frequencies of each TAP genes. Our result suggests that TAP1 and TAP2 gene are not primarily involved in the pathogenesis of Japanese BD. However, the weak association between allele frequency of TAP2C and erythema nodosum indicates the possibility that TAP2C may be associated with the formation of erythema nodosum, specific symptom of BD. Our result supports the possibility that the existence of TAP2C influences merely on formation of erythema nodosum, because the difference became indistinct, when the patients who had at least one kind of skin lesion (including erythema nodosum, subcutaneous thrombophlebitis, folliculitis and cutaneous hypersensitivity) were compared with controls. Further study about peptide fragment which is translocated from the cytosol to the ER by TAP2, would make elucidation of pathogenesis of erythema nodosum in BD possible.

We observed increased frequency of HLA-B*5101 in Japanese patients with BD and the tendency was still significant even if p value was corrected. Considering the presence of many studies [18,19] which similarly report the correlation between HLA-B*5101 and BD, HLA-B51 is the most plausible candidate of susceptibility. However, it is not clarified whether the HLA-B51 itself is the primary susceptibility factor of BD or some other gene in a linkage disequilibrium to HLA-B51 is involved in the pathogenesis of the disease.

We observed a high frequency of TAP2C allele in HLA-B*5101 positive patients with BD compared with HLA-B*5101 negative patients, even though this difference did not reach statistical significance. There remains the problem whether this result is caused by linkage disequilibrium between TAP2 and HLA-B51 or not. Ishihara *et al.*[20] have reported that they observed no linkage disequilibrium between TAP2*0101 and HLA-B51. (TAP2*0101 correspond to the total of TAP2A and TAP2C in our context) Making use of their result, the presence of TAP2C might be involved in the formation of erythema nodosum independently of the HLA-B*5101.

Although Gonza'lez-Escribano *et al.*[11] showed an absence of phenotype frequency of TAP1C in the patients with BD by ARMS-PCR method, we observed low phenotype frequency of TAP1C not merely in the patients with BD (4.3%) but also in Japanese normal subjects (0%). We suppose that the low frequency of TAP1C in Japanese BD was caused by ethnical background of Japanese independently of pathogenesis of BD (Table IV).

Additionally, our results of phenotype and genotype frequency of TAP2 indicate the relation between TAP2H and skin lesion of BD. In order to clarify their susceptibility, further study is required which analyses their frequency classifying the patients who have skin lesion into each symptom.

In HLA class II typing, we observed a high frequency of HLA-DR6 in patients with BD. Although the disease associations with HLA class II are generally considered weaker and more complex than those seen with HLA-B51, some studies[17,21] have already reported high frequency of HLA-DR6 in patients and Jorizzo[22] has reported that HLA-DR1 and HLA-DQw1 positive patients might have an innate resistance to the development of BD. Our result confirms the association of HLA-DR6 with BD.

As previously reported,[23] not only the genetic background but also environmental factors may play some part in the pathogenesis of BD. The biological and genetic mechanisms underlying the pathogenesis of BD are still indistinct. The hypothesis that the presence of TAP2C allele is involved in the formation of erythema nodosum in BD is interesting and requires further study.

Acknowledgements

We acknowledge kind advices of Dr Katsushi Tokunaga in University of Tokyo, and the cooperation of Dr Atsuko Ogawa in Japanese Red Cross Central Blood Center.

References

[1] Ehrlich, G.E. (1989) "Behçet's disease: current concepts", *Compr. Ther.* **15**, 27–30.
[2] Ohno, S., Aoki, K., Sugiura, S., Nakayama, E., Itakura, K. and Aizawa, M. (1973) "HL-A5 and Behçet's disease", *Lancet* **2**, 1383–1384.
[3] Ohno, S., Asanuma, T., Sugiura, S., Wakisaka, A. and Aizawa, M. (1978) "HLA-Bw51 and Behçet's disease", *J. Am. Med. Assoc.* **240**, 529.

[4] Yazici, H., Chamberlain, M.A., Schreuder, I., D'Amaro, J. and Muftuoglu, M. (1980) "HLA antigens in Behçet's disease: a reappraisal by a comparative study of Turkish and British patients", *Ann. Rheum. Dis.* **39**, 344–348.

[5] Ohno, S., Ohguchi, M., Hirose, S., Matsuda, H., Wakisaka, A. and Aizawa, M. (1982) "Close association of HLA-Bw51 with Behçet's disease", *Arch. Ophthalmol.* **100**, 1455–1458.

[6] Sakane, T. and Miura, K. (1996) "Research for basic and clinical aspects of Behçet's disease—recent advance and future", *Nippon-Rinsho* **54**, 870–884.

[7] Sun, A., Lin, S.C., Chu, C.T. and Chiang, C.P. (1993) "HLA-DR and DQ antigens in Chinese patients with Behçet's disease", *J. Oral Pathol. Med.* **22**, 60–63.

[8] Spies, T., Cerundolo, V., Colonna, M., Cresswell, P., Townsend, A. and DeMars, R. (1992) "Presentation of viral antigen by MHC class_molecules is dependent on a putative peptide transporter heterodimer", *Nature* **355**, 644–646.

[9] Shepherd, J.C., Schumacher, T.N., Ashton-Rickardt, P.G., Imaeda, S., Ploegh, H.L., Janeway, C.A., Jr, *et al.* (1993) "TAP1-dependent peptide translocation *in vitro* is ATP dependent and peptide selective", *Cell* **74**, 577–584.

[10] Powis, S.H., Tonks, S., Mockridge, I., Kelly, A.P., Bodmer, J.G. and Trowsdale, J. (1993) "Alleles and haplotypes of the MHC-encoded ABC transporters TAP1 and TAP2", *Immunogenetics* **37**, 373–380.

[11] Gonza'lez-Escribano, M.F., Morales, J., Garcia-Lozano, J.R., Castillo, M.J., Sanchez-Roman, J., Nunez Roldan, A., *et al.* (1995) "TAP polymorphism in patients with Behçet's disease", *Ann. Rheum. Dis.* **54**, 386–388.

[12] Kuwata, S., Yanagisawa, M., Saeki, H., Nakagawa, H., Etoh, T., Tokunaga, K., *et al.* (1995) "Lack of primary association between transporter associated with antigen processing genes and atopic dermatitis", *J. Allergy Clin. Immunol.* **96**, 1051–1060.

[13] Takeuchi, F., Kuwata, K., Nakano, K., Nabeta, H., Hong, G.H., Shibata, Y., *et al.* (1996) "Association of TAP1 and TAP2 with systemic sclerosis in Japanese", *Clin. Exp. Rheumatol.* **14**, 513–521.

[14] Saiki, R.K., Gelfand, D.H., Stoffel, S., Scharf, S.J., Higuchi, R., Horn, G.T., *et al.* (1988) "Primer-directed enzymatic amplification of DNA with a thermostable DNA polymerase", *Science* **239**, 487–491.

[15] Powis, S.H., Rosenberg, W.M., Hall, M., Mockridge, I., Tonks, S., Ivinson, A., *et al.* (1993) "TAP1 and TAP2 polymorphism in coeliac disease", *Immunogenetics* **38**, 345–350.

[16] Bannai, M., Tokunaga, K., Lin, L., Ogawa, A., Fujisawa, K. and Juji, T. (1996) "HLA-B40, B18, B27, and B37 allele discrimination using group-specific amplification and SSCP method", *Human Immunol.* **46**, 107–113.

[17] Tokunaga, K., Ishikawa, Y., Ogawa, A., Wang, H., Mitsunaga, S., Moriyama, S., *et al.* (1997) "Sequence-based association analysis of HLA class_and_alleles in Japanese supports conservation of common haplotypes", *Immunogenetics* **46**, 199–205.

[18] Mizuki, N., Inoko, H., Mizuki, N., Tanaka, H., Kera, J., Tsuji, K., *et al.* (1992) "Human leukocyte antigen serologic and DNA typing of Behçet's disease and its primary association with B51", *Investig. Ophthalmol. Vis. Sci.* **33**, 3332–3340.

[19] Mizuki, N., Inoko, H., Ando, H., Nakamura, S., Kashiwase, K. and Akaza, T. (1993) "Behçet's disease associated with one of the HLA-B51 subantigens, HLA-B*5101", *Am. J. Ophthalmol.* **116**, 406–409.

[20] Ishihara, M., Ohno, S., Mizuki, N., Yamagata, N., Naruse, T., Shiina, T., *et al.* (1996) "Allelic variations in the TAP2 and LMP2 genes in *Behçet's disease*", *Tissue Antigens* **47**, 249–252.

[21] Sasazuki, T., Nishimura, Y., Mineshita, S., Miyashita, H. and Inaba, G. (1982) "Genetic analysis of Behçet's disease", In: Inaba, G., eds, *Behçet's Disease* (University of Tokyo Press, Tokyo), pp 33–40.

[22] Jorizzo, J.L. (1986) "Behçet's disease. An update based on the 1985 International Conference in London", *Arch. Dermatol.* **122**, 556–558.

[23] Hirohata, T., Kuratsune, M., Nomura, A. and Jimi, S. (1975) "Prevalence of Behçet's syndrome in Hawaii", *Hawaii Med. J.* **34**, 244–246.

[24] Wordsworth, B.P., Pile, K.D., Gibson, K., Burney, R.O., Mockridge, I. and Powis, S.H. (1993) "Analysis of the MHC-encoded transporters TAP1 and TAP2 in rheumatoid arthritis: linkage with DR4 accounts for the association with a minor TAP2 allele", *Tissue Antigens* **42**, 153–155.

Rheumatol Int (2003) 23: 315–318
DOI 10.1007/s00296-003-0310-7

CASE REPORT

M. Takayanagi · H. Haraoka · H. Kikuchi · S. Hirohata

Myocardial infarction caused by rheumatoid vasculitis: histological evidence of the involvement of T lymphocytes

Received: 24 September 2002 / Accepted: 23 January 2003 / Published online: 21 March 2003

Abstract Rheumatoid arthritis (RA) is a chronic joint disease that can be complicated with extra-articular manifestations due to vasculitis. We describe a patient with RA who developed systemic vasculitis and died of myocardial infarction. Autopsy demonstrated vasculitis of the left anterior descendent and circumflex coronary arteries, which were narrowed or occluded with organizing thrombosis. Formation of granuloma with multinucleated giant cells was also observed in media of the circumflex artery. There was no microscopic evidence of atheroma formation in the coronary arteries. Of note, there was a follicle-like infiltration of CD45RO-positive T lymphocytes in interna of the left coronary arteries and the right renal artery. Although not frequently reported, coronary vasculitis as a cause of myocardial infarction should be considered in patients with RA. Moreover, our results suggest that infiltration of T lymphocytes might be involved in the development of rheumatoid vasculitis.

Keywords CD45RO · Coronary artery · Rheumatoid arthritis · T lymphocytes · Vasculitis

Introduction

A variety of extra-articular manifestations have been found to occur in patients with rheumatoid arthritis (RA), including subcutaneous nodules, episcleritis, mononeuritis multiplex, serositis, petechiae, and skin ulcers. Several of these manifestations are considered to originate from systemic vasculitis, which has been reported to result in mortality rates as high as 30% [1, 2, 3]. On the other hand, coronary vasculitis as a cause of myocardial infarction has rarely been reported in RA patients [4, 5, 6, 7, 8]. However, review of the autopsy material of 169 patients with RA revealed that coronary arteritis with multiple cardiac infarction was the direct cause of death in ten cases (5.9%) [9]. Therefore, coronary vasculitis is not as rare as has been expected. Although there have been a few reports on definite fatal coronary arteritis in RA [6, 7, 8], either the pathogenesis or the histological characteristics have not been clearly delineated. In this report, we describe an RA patient who died of myocardial infarction secondary to rheumatoid vasculitis, proven by autopsy. More importantly, immunohistological analysis disclosed a follicle-like infiltration of CD45RO-positive T lymphocytes in interna of branches of the left coronary artery, which might be involved in the development of the vasculitis.

M. Takayanagi · H. Haraoka · H. Kikuchi · S. Hirohata (✉)
Department of Internal Medicine,
Teikyo University School of Medicine,
2-11-1 Kaga, Itabashi-ku, Tokyo 173-8605, Japan
E-mail: shunsei@med.teikyo-u.ac.jp
Tel.: +81-3-39641211 ext 1568
Fax: +81-3-39647094

Case report

A 74-year-old man had been in good health until October 1998, when he developed stiffness and painful swelling in his shoulders, knees, and hands, with mild elevation of serum rheumatoid factor (rheumatoid arthritis particle agglutination, or RAPA, 1:40, normal < 40). He was diagnosed with RA according to 1987 American College of Rheumatology criteria [10]. Laboratory tests at that time revealed erythrocyte sedimentation rate (ESR) (Westergren) of 98 mm/h and C-reactive protein (CRP) at 9.3 mg/dl. Thus, treatment with prednisolone (7.5–15 mg/day), nonsteroidal anti-inflammatory drugs, and sulfasalazine (1 g/day) was started. However, the patient developed subcutaneous nodules along with exacerbation of the polyarthritis in July 1999. Laboratory tests at this time showed ESR 115 mm/h, CRP 10.6 mg/dl, and RAPA 1:2560. In August 1999, sulfasalazine was discontinued and D-penicillamine (100 mg/day) was started. On August 27, 1999, the patient suddenly noted right visual disturbances. Ophthalmological examinations revealed no abnormalities in optic fundus, lens, iris, or anterior sclera of the right eye. He was admitted to the Department of Ophthalmology of our hospital for evaluation on September 29, 1999 and diagnosed after extensive ophthalmological examination as having retrobulbar optic neuritis. He recovered sight after treatment with intravenous alprostadil (prostaglandin E1) for 7 days, followed by therapy with intravenous administration of

methylprednisolone (1 g/day) for 3 consecutive days. However, he developed fever with pulmonary infiltration on November 3 and was admitted to our department on November 5, 1999.

On admission, physical examination showed wheezing over his chest wall. Laboratory data showed a white blood cell count of 23.6×10^9/l with 20% band forms and 71% segment forms, CRP 20.16 mg/dl, RAPA 1:2560, total hemolytic complement 23 U/ml (normal 29–41 U/ml), and circulating immune complex 5.0 μg Eq/ml by C1q binding assay (normal < 3.0). Antinuclear antibody and antineutrophil cytoplasmic antibody were both negative. Chest X-ray revealed diffuse pulmonary infiltrates in the lower lobe of the right lung. The patient was thus diagnosed with bronchopneumonia, and treatment with antibiotics was started. Although recovering from the pneumonia, he presented a minor attack of myocardial infarction, as evidenced by a transient elevation of creatine kinase and STT changes in electrocardiography on November 10, which improved in 3 days with conservative treatment. However, he died suddenly of heart arrest on November 18, 1999.

Postmortem examinations revealed a well localized area of yellow discoloration in the left lateral ventricular wall and the septum. Macroscopically, the anterior descending artery was almost patent, but the circumflex artery was almost totally occluded without characteristics of atheroma or calcification. Microscopically, a cross-section of the circumflex artery showed occlusion of the lumen with organizing thrombus and fibrinoid necrosis, infiltration of mononuclear cells in all three layers, and formation of granuloma with multinucleated giant cells in media (Fig. 1). Of note, there was follicle-like infiltration of CD45RO-positive T lymphocytes but no CD20-positive B lymphocytes or CD68-positive monocytes (data not shown) in interna of the circumflex coronary artery (Fig. 2A, B). The anterior descending artery showed only narrowing of the lumen with thickening of interna, whereas the follicle-like infiltration of CD45RO-positive T lymphocytes was more marked than in the circumflex artery (Fig. 2C, D). Moreover, similar follicle-like infiltration of CD45RO-positive T lymphocytes was also demonstrated in interna and media of the right renal artery (Fig. 3). There was no microscopic evidence of atheroma formation in the coronary arteries. Taken together, these findings demonstrate that the myocardial infarction in our patient was caused by rheumatoid vasculitis. In addition, the results of immunohistological staining indicated that infiltration of activated T lymphocytes was involved in the development of not only coronary arteritis but systemic vasculitis.

Fig. 1A–B Cross-section of the circumflex artery. The lumen is occluded with organizing thrombus and fibrinoid necrosis, and all three layers are infiltrated with mononuclear cells (A) and formation of granuloma with multinucleated giant cells in media (B). H&E staining, original magnification of A ×10, of B ×50

Discussion

Recent studies clearly demonstrated that the incidence of cardiovascular events in RA patients is higher, independently of traditional cardiovascular risk factors, presumably from accelerated atherosclerosis due to a wide range of inflammatory mechanisms [11, 12]. Since the incidence of coronary vasculitis has been found to be relatively high [9], it is possible that it might also be a risk factor for the more frequent cardiovascular events in RA patients. Of note, the circumflex coronary artery of our patient proved to be occluded by organizing thrombus with fibrinoid necrosis due to inflammatory lesions without the presence of atherosclerosis. In fact, our patient had no risk factors for atherosclerosis. Moreover, formation of granuloma with multinucleated giant cells was also observed in media of the circumflex coronary artery of our patient. It is therefore most likely that his myocardial infarction was caused by necrotizing granulomatous vasculitis secondary to RA. In fact, there have been a few reports on cases with histological evidence of rheumatoid vasculitis that lead to myocardial infarction without atherosclerosis [6]. Taken together, these observations confirm that coronary vasculitis as a cause of myocardial infarction should be considered in patients with RA unless accompanied by risk factors for atherosclerosis.

Similarly to other cases with histopathologically proven coronary vasculitis as the cause of myocardial infarction [6, 7, 8], our patient had progressive rheumatoid disease and subcutaneous nodules with marked elevation of serum rheumatoid factors, increased levels of circulating immune complex, and hypocomplementemia. Of note, he suffered from retrobulbar optic neuritis prior to developing myocardial infarction. There have been several reports that optic neuritis might be induced by vasculitis in RA [13, 14]. It is therefore likely that retrobulbar optic neuritis is one of the manifestations of rheumatoid vasculitis in this case. In this regard, our patient had risk factors for the development of myocardial infarction due to rheumatoid vasculitis, as was suggested in the previous study [6, 7].

Several studies have reported the histopathological features of coronary vasculitis due to RA, including intense mononuclear cell infiltration of all three layers, narrowing of the lumen with fibroblastic proliferation,

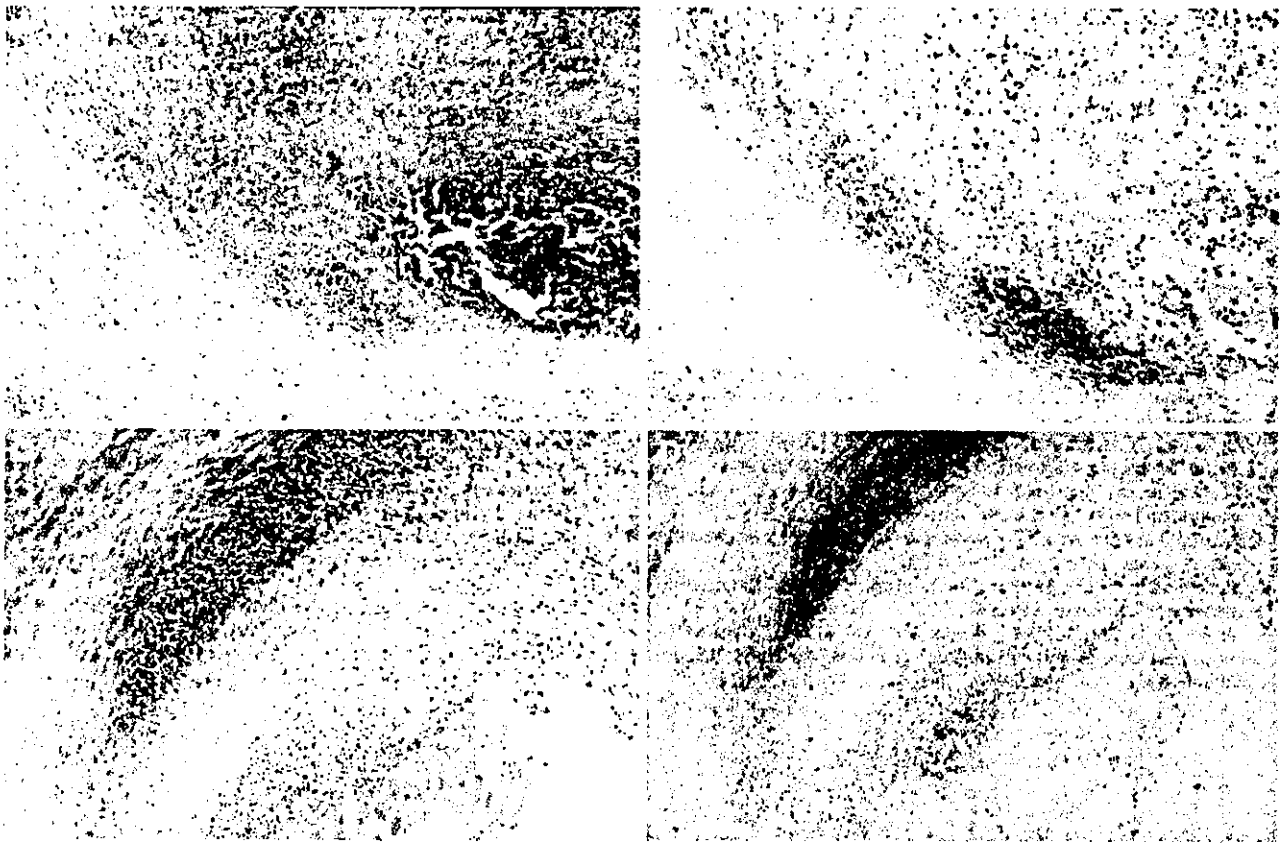

Fig. 2A–D Cross-sections of the circumflex artery (A, B) and the anterior descending artery (C, D). A, C The follicle-like infiltration of CD45RO-positive T lymphocytes is observed in interna (H&E, original magnification ×25). B, D Immunohistological staining of paraffin-embedded section with UCHL-1 (anti-CD45RO) followed by counterstaining with peroxidase-conjugated goat antimouse IgG. Original magnification ×25

fibrinoid necrosis, and organizing thrombus [4, 5, 6, 7, 8]. In addition to these features, the present study disclosed the formation of granuloma with multinucleated giant cells in the circumflex coronary artery. More importantly, a follicle-like infiltration CD45RO-positive T lymphocytes was demonstrated in interna of the circumflex and anterior descending coronary arteries. This infiltration was more marked in the anterior descending coronary artery, where the occlusive changes were less marked. It is therefore likely that such infiltration might take place in the early stage of vasculitis and thus trigger the occurrence of rheumatoid vasculitis. Of note in our patient, follicle-like infiltration of CD45RO-positive T lymphocytes was also observed in interna and media of the right renal artery. It is thus suggested that memory T lymphocytes might be involved in the

▶

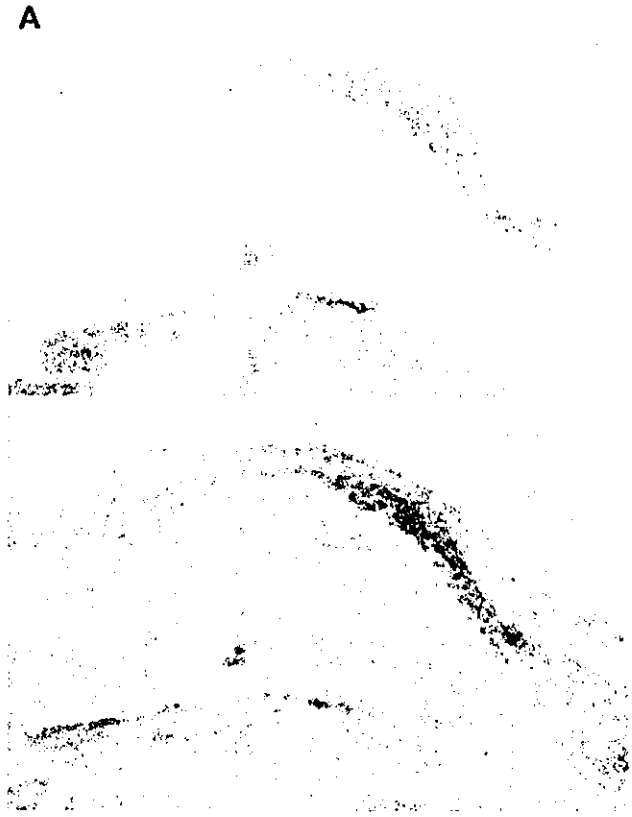

Fig. 3A–B Longitudinal section of the right renal artery. A The follicle-like infiltration of CD45RO-positive T lymphocytes is observed in interna and media. H&E, original magnification ×10. B Immunohistological staining of paraffin-embedded section with UCHL-1 (anti-CD45RO) followed by counterstaining with peroxidase-conjugated goat antimouse IgG. Original magnification ×10

development of not only coronary vasculitis but systemic vasculitis in RA. Further studies to delineate the clonality and antigen specificity of these T lymphocytes would be important in ascertaining mechanisms of the development of rheumatoid vasculitis.

Acknowledgement This work was supported by a grant from Manabe Medical Foundation, Tokyo, Japan. The author wish to thank Dr. Mamoru Kosakai for his help in pathological examination.

References

1. Scott DGI, Bacon PA, Tribe CR (1981) Systemic rheumatoid vasculitis. A clinical and laboratory study of 50 cases. Medicine (Baltimore) 60:288–297
2. Bywaters EGL, Scott JT (1963) The natural history of vascular lesions in rheumatoid arthritis. J Chron Dis 16:905–914
3. Wilkinson M, Torrance WN (1967) Clinical background of rheumatoid vascular disease. Ann Rheum Dis 26:475–479
4. Karten I (1969) Arteritis, myocardial infarction and rheumatoid arthritis. JAMA 210:1717–1720
5. Sweezy RL (1967) Myocardial infarction due to rheumatoid arthritis. JAMA 199:855–857
6. Voyles WF, Searles RP, Bankhurst AD (1980) Myocardial infarction caused by rheumatoid vasculitis. Arthritis Rheum 23:860–863
7. Van Albada-Kuipers GA, Bruijn JA, Westedt M-L, Breedveld FC, Eulderink F (1986) Coronary arteritis complicating rheumatoid arthritis. Ann Rheum Dis 45:963–965
8. Morris PB, Imber MJ, Heinsimer JA, Hlatky MA, Reimer KA (1986) Rheumatoid arthritis and coronary arteritis. Am J Cardiol 57:689–691
9. Bely M, Apathy A, Beke-Martos E (1992) Cardiac changes in rheumatoid arthritis. Acta Morphol Hung 40:149–186
10. Arnett FC, Edworthy SM, Bloch DA, McShane DJ, Fries JF, Cooper NS, Healey LA, Kaplan SR, Liang MH, Luthra HS, Medsger TA Jr, Mitchell DM, Neustadt DH, Pinals RS, Schaller JG, Sharp JT, Wilder RL, Hunder GG (1988) The American Rheumatism Association 1987 revised criteria for the classification of rheumatoid arthritis. Arthritis Rheum 31:315–324
11. del Rincón I, Williams K, Stern MP, Freeman GL, Escalante A (2001) High incidence of cardiovascular events in a rheumatoid arthritis cohort not explained by traditional cardiac risk factors. Arthritis Rheum 44:2737–2745
12. Wolfe F, Freundlich B, Straus WL (2003) Increase in cardiovascular and cerebrovascular disease prevalence in rheumatoid arthritis. J Rheumatol 30:36–40
13. Sklar EM, Schatz NJ, Glaser JS, Post MJ, ten Hove MO (1996) MR of vasculitis-induced optic neuropathy. Am J Neuroradiol 17:121–128
14. Yucel AE, Kart H, Aydin P, Agildere AM, Benli S, Altinors N, Demirhan B (2001) Pachymeningitis and optic neuritis in rheumatoid arthritis: successful treatment with cyclophosphamide. Clin Rheumatol 20:136–139

総 説

ウイルスとリウマチ性疾患

三田村 巧[1] 武井 正美[1] 澤田 滋正[1,2]

[1]日本大学医学部内科学講座内科1部門
[2]日本大学練馬光が丘病院内科

Viruses in Rheumatic Disease

Ko Mitamura[1], Masami Takei[1] and Shigemasa Sawada[1,2]

[1] *First Department of Internal Mdicine, Nihon University School of Medicine*
[2] *Nerima Hikarigaoka Nihon University Hospital*

Various genetic factors and environmental factors are intricately intertwined in the pathomechanism of rheumatic diseases. An infectious cause has long been postulated to explain the development of autoimmunity. Several study groups demonstrated viral structures exist in the target tissues. We have also reported the expression of Epstein-Barr virus (EBV) DNA, RNA or associated proteins in synovial tissue specimens or synovial cells from patients with RA. And recent progress in molecular biology reveal mechanism caused by viruses in the diseases. Infections of target tissues could result in the release or expression sequestered antigens or in the ability to present self antigens that are normally prevented from being exposed to the immune system. Molecular mimicry is one mechanism by which infectious agents may trigger an immune response against autoantigens. In this review, we describe the relationship between viruses and rheumatic diseases as autoimmune diseases.

Key words: virus, rheumatic diseases, autoimmunity, Epstein-Barr virus, molecular mimicry
ウイルス，リウマチ性疾患，自己免疫，EBウイルス，分子相同性

(J. Nihon Univ. Med. Ass., 2003; 62 (12): 633-638)

はじめに

リウマチ性疾患・自己免疫疾患の発症には，遺伝的因子を背景にして環境因子により，免疫学的自己寛容の破綻をおこすことが，重大な要因と考えられている．この環境因子の中の病原微生物とリウマチ性疾患・自己免疫疾患との関わりとしては，

①微生物が直接関節内に入った場合は感染性関節炎となり，急性炎症を引き起こす．②しかし必ずしも微生物が直接証明されず，腸管感染症や尿道炎後に起こる反応性関節炎といわれる関節炎も存在する．Salmonella, Sigella, Campylobacterなどの腸管感染症やChlamydiaによる尿道炎後に，主にHLA-B27陽性者に起こる関節炎である．これは免疫反応が微生物に反応するとともにHLA-B27との交差反応性と分子相同性 (molecular mimicry) の仮説が関節炎の引き金となると考えられている[1]．リウマチ性疾患・自己免疫疾患の発症と病態に関与する病原微生物のなかでも主にウイルスとリウマチ性疾患の関わりにつきこの総説においては述べる．

I. ウイルス感染

ウイルスの急性感染においては，しばしば急性の単～多発性関節炎をおこす．一過性で対称性の可逆性の関節炎のことが多い．風疹ウイルス，インフルエンザウイルス，パルボウイルスB19，B型肝炎ウイルス，C型肝炎ウイルス，ヒトT細胞白血病ウイルス (HTLV-1)，HIVなどがこれにあたる．ウイルス感染による免疫複合体生成の際や炎症性サイトカインの産生により関節炎が出現すると考えられている．

またウイルス感染に伴い一過性に抗核抗体が出現することもよく知られており，健康小児に抗核抗体が陽性である場合には注意が必要である．近年自己抗原の分子構造が明らかになり，ウイルスの自己抗体産生への関与が解明されつつある．例えば，ウイルス蛋白と自己抗原エピトープが共通したアミノ酸配列を持つことにより，抗ウイルス抗体が交差反応により自己抗体として誘導される，またある種のウイルスRNAは自己抗原リボ核蛋白と結合し，自己抗原蛋白が修飾され自己抗体が産生され

受付：2003年11月26日， 受理：2003年12月25日

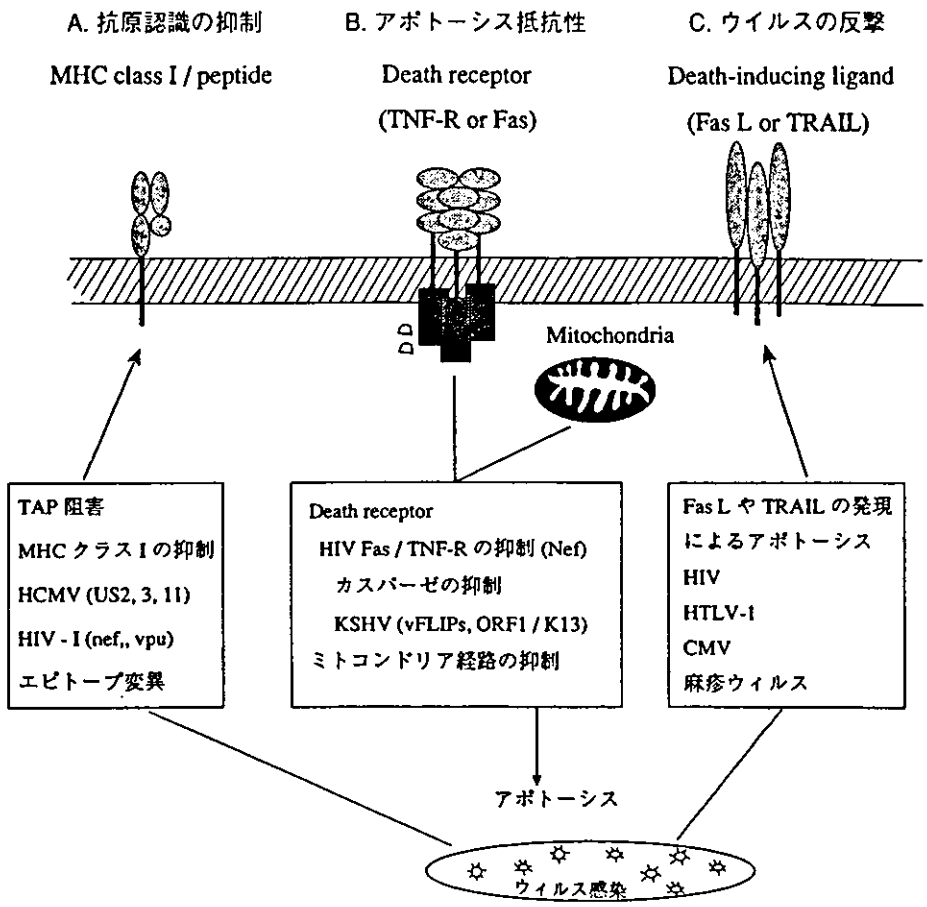

Fig. 1 Evasion of immune responses by viruses in human major mechanisms used by viruses to evade immune responses in human are illustrated. (文献[2]より)

るなどという考えである.

ウイルス感染が一過性でなく，生体の免疫機構から逃れウイルスの持続感染や再活性化が成立した場合には，遺伝的因子を背景にして，分子相同性などによる自己免疫反応が起こり，免疫学的自己寛容の破綻をおこしリウマチ性疾患が発症すると考えられる.

それでは，いかにしてウイルスの持続感染の成立がなされるであろうか？ つぎに持続感染の成立の機構につき解説する.

II. ウイルスの持続感染の成立機構

一般に生体内でウイルス感染がおこると，ウイルス由来抗原は細胞質内で分解され，transporter in antigen processing (TAP) により粗面小胞体に移送され，β2-ミクログロブリンとによりMHCクラスIと結合しゴルジ装置に運ばれ，エクソサイトーシスにより細胞表面に表現される．その分子を標的にしてウイルス抗原特異的な細胞障害性T細胞 (CTL) が誘導され，パーフォリンやFas依存性の機構によりウイルス感染細胞の排除が試みられる．一方ウイルス側ではこれらから逃れるために，蛋白を合成し，感染した細胞の性質を変化させウイルス排除より免れようとし，以下の働きを試みる[2].

A：抗原認識の抑制：細胞表面への提示過程で，TAP機能を抑制する蛋白 *US2,3,11* を合成し粗面小胞体への移送を抑制し抗原認識から逃れる (human cytomegalovirus HCMV)[3]. Human immunodeficiency virus (HIV) は，nef蛋白合成によりMHC class Iの発現抑制を行い，また突然変異によるウイルス抗原そのものを変化させたりすることによりCTLの抗原認識を抑えようとする[4].

B：アポトーシス抵抗性：ウイルス産生蛋白により感染細胞のアポトーシスを抑制する．それは，細胞表面のTNF receptor familyを介したアポトーシスの抑制 (HIV の *nef*) や，Bcl-2 familyによるミトコンドリア内での過程を抑制するもので，これらはともにアポトーシスを誘導するcaspases活性化の抑制を介する制御をおこなっている (HIV, Kaposi's sarcoma-associated herpesvirus: KSHV による vFLIP といわれる caspases 8 抑制因子[5], EBV 等).

C：ウイルスの反撃：FasL や TRAIL を介して，ウイルス抗原を認識した CTL を逆にアポトーシスを起こさせ，CTL からの攻撃に反撃をする (HIV[6], HTLV-1, CMV, 麻疹ウイルス等) (Fig. 1).

これ等の機構により，ウイルスはヒトのウイルス排除の免疫機構から逃れ感染を存続させ，リウマチ性疾患・

自己免疫疾患の出現に関与することが解明されつつある．

次に具体的にいくつかのウイルスとの関連を指摘されている疾患について解説していく．

III. ウイルスと種々の疾患

1. パルボウイルス B19

パルボウイルス B19 は，DNA ウイルスの一種でヒトに病原性を持つ唯一のパルボウイルスである．一般にパルボウイルス B19 の感染は無症状ですむことが多い．小児では伝染性紅斑症を起こすウイルスとして有名である．りんご病と言われるように，その顔面の皮疹は全身性エリテマトーデス (SLE) 様の紅斑である．成人の急性感染では多発性関節炎をよくひきおこし，皮疹を欠くことが多く，関節の腫脹と朝のこわばりを伴い関節リウマチ (RA) 様である．1～2 週間で関節炎はおさまることが多いが，数カ月から数年にもわたり遷延することもある．妊婦が初期～中期に感染すると胎児水腫を起こし流産となることがある．また骨髄での赤芽球系細胞への感染により赤芽球癆や再生不良性貧血をきたすことがある．また報告例のなかには，高熱と関節炎で発症し，白血球減少，クームス陽性の溶血性貧血，血小板減少，自己抗体陽性，anti-dsDNA 抗体陽性，低補体価が出現し，当初SLEの診断基準を満たし，SLE としてステロイド治療がおこなわれた症例も報告されている[7]．その他に成人スチル病[8]の血中や，皮膚筋炎／多発筋炎の筋組織[9]，強皮症の骨髄[10]でも PCR 法にて検出されている．また血球貪食症候群[11]を発症した例の報告もあり，様々な疾患との関わりが論じられている．しかしこれらの多くは持続感染と病因との関連を証明したものではなく，病因としてのパルボウイルス B19 の関与の解明は今後の研究が待たれる．一方，RA の病因としてのパルボウイルス B19 が最近注目され沢山の研究が報告されている．急性感染後の数カ月から数年にもわたり多発性関節炎が遷延化し，滑膜増殖と骨びらんを伴う典型的な RA を発症する例が報告されている[12]．Sasaki 等は RA 関節滑膜においてのみ B19RNA，B19 蛋白 VP-1 が検出でき，RA 関節滑膜のみ B19 が活性化し持続感染を引き起こしたと報告している[13]．また患者の関節滑膜だけでなく骨髄にもウイルス DNA と VP-1 が長期に存在し，DMARDs 治療抵抗性となったためγグロブリン大量療法を施行したところ，臨床症状の改善と骨髄での VP-1 陽性細胞の減少が認められたと報告されている．さらに B19 蛋白 VP-1 は，RA 滑膜に浸潤している T 細胞，B 細胞，マクロファージ，濾胞樹状細胞に陽性であり，滑膜表層細胞，好中球，血管内皮細胞には認めなかった[13]．RA 滑膜細胞からマクロファージ様細胞株 U937，THP-1 に感染させることができ，それらの細胞の TNF-α，IL-6 の産生を誘導した．パルボウイルス B19 の非構造蛋白 NS1 は，NF-κB の活性化を介し IL-6 遺伝子の発現増強作用があり，アポトーシスを誘導する[14]．今まではパルボウイルス B19 は，赤血球型抗原である p 抗原をレセプターとして赤芽球系細胞への感染することしか明確でなかったが[15]，免疫担当細胞への感染が明らかにされ炎症性サイトカインの産生亢進やアポトーシスを誘導することが明らかにされ，リウマチ性疾患・自己免疫疾患への病因関与の可能性につながるものである．

2. Epstein-Barr ウイルス

(1) RA と EBV

EBV は伝染性単核球症を引き起こし，初感染後ホストに潜在化することが知られており，リウマチ性疾患との関わりが以前より指摘されている．Alspaugh 等は RA 患者末梢血中に EBV 感染細胞核成分に対する抗体：RA nuclear antigen 抗体 (RANA) を発見している[16]．その後 RANA 抗体が認識する主なエピトープは，EBNA (EBV determined nuclear antigen)-1 の glysine-alanine 構造であることが判明した[17]．また RA 滑膜には，EBNA-1 と一部構造が似ている蛋白が報告されている[18]．

RA 関節滑膜細胞に存在する EBV

我々は，*in situ* hybridization 法により RA 滑膜 34 例中 8 例 (23.5%) に EBV encoded small RNA (EBER)-1 を検出した．変形性関節症の滑膜 20 例の検討では全例陰性であった ($p < 0.05$)．RA 滑膜における EBER-1 の発現部位は，滑膜細胞が絨毛上に増殖のみられる先端のところで陽性であった．EBV 関連抗原 latent membrane protein-1 (LMP-1) の発現は，同一患者の EBER-1 の発現部位に一致した[19]．Takeda 等も RA 滑膜細胞での EBER-1 や EBV DNA の発現を報告し[20]，岩田，立石等は RA 軟骨下骨部の単核球に EBV の存在を *in situ* hybridization 法，免疫組織染色での LMP-1 の発現滑膜細胞の存在を証明した (第 43 回日本リウマチ学会総会 F84-4, 1999)．

RA 関節滑膜細胞への EBV 感染成立機序

EBV のレセプターとしては CD21 (C3d レセプター) が知られているが，EBV 陽性 RA 滑膜表層細胞は CD21 陰性であった．近年注目されている EBV 陽性上咽頭癌，胃癌細胞も CD21 陰性であり，その感染機序は明らかではない．Hirohata 等は，RA または変形性関節症 (OA) 骨髄由来 CD34 陽性細胞を分離し，EBV 陰性患者 B 細胞と共存培養することで RA 骨髄由来の CD34 細胞共存培養の系からは EBV 陽性細胞株を樹立できたが，OA のものからは得られなかったと報告した[21]．我々は，Hirohata 等が樹立した B 細胞株と患者唾液由来の EBV 野生株のウイルス株において，EBNA3c の DNA 配列を決定することにより，塩基の変異や繰り返し構造が一つの塩基変異を除いて完全に一致したことを明らかにした．これは RA 骨髄のある微小環境が EBV の感染に強

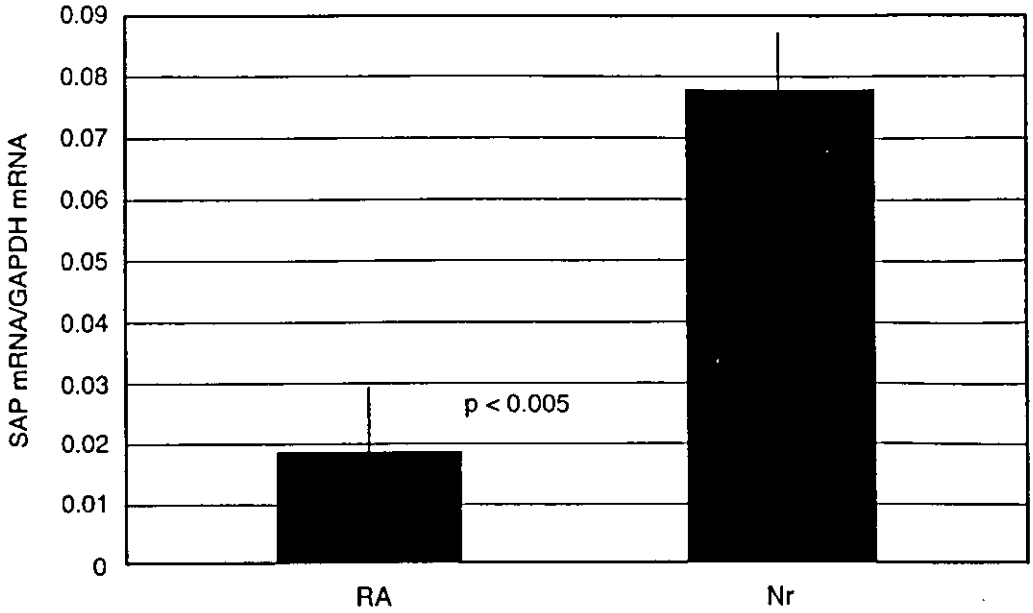

Fig. 2 The expression level of SAP transcripts in peripheral $CD2^+$ T cell of RA patients is decreased. The expression level of SAP transcripts normalized with that of GAPDH transcripts in $CD2^+$ T cells is indicated. The expression level of SAP transcripts in peripheral $CD2^+$ T cells of five RA patients (0.0182 ± 0.011) was significantly lower than that of five normal individuals (0.0779 ± 0.01) ($p < 0.005$, RA patients versus normal, Student's t-test). Values are mean ± SD.

く関与し，何処かで感染した非リンパ球系の細胞が例えば骨髄よりリクルートされ絨毛上に増殖する可能性を見い出した(第44回日本リウマチ学会総会シンポジウム，2000)．Blaschke 等は滑膜細胞の単層の表層細胞の直下に EBV 陽性の細胞が集簇していることを EBER-1/2 の in situ hybridization 法で報告した[22]．この発見は前述した仮説を裏付ける可能性があり滑膜の多層性の絨毛状に増殖する過程を捉えているとも考えられる．

RA での EBV に対するホストデイフェンスの異常

EBV の EBER-1, LMP-1 が滑膜表層細胞の最も増殖を起こしている場所と推定される部位に発現していたが，LMP-1 は細胞障害性 T 細胞の標的分子であり，通常の免疫機能を有していれば個体から排除されてしまう．RA 滑膜で EBV 感染細胞が排除されず存在する機構の原因は不明であった．

我々が協和発酵東京研究所の石渡博士らとの IgA 腎症の共同研究において発見した遺伝子 (国際公開番号：WO98-24899, H8. 12. 5) は，小児期に EBV の致死的感染症を起こすことで知られている Duncan 病 (X-linked lymphoproliferative syndrome: XLP) の原因遺伝子である signaling lymphocytic-activation molecule (SLAM) associated protein (SAP)[23] と同一遺伝子であった．Duncan 病は，この遺伝子異常や発現の低下により EBV に対する特異的抑制性 T 細胞の誘導ができないと考えられている．RA 患者末梢血 T 細胞において real time PCR 法にて，SAP mRNA の発現は正常者に比較し有意に低下を示した (Fig. 2)．しかし，5 例の RA 患者末梢白血球からの SAP cDNA には全く変異を認めなかった．RA で EBV に対する感染防御機構が機能せず，滑膜での持続感染を起こす原因として，SAP 分子の発現異常が関与する可能性がある[24]．

(2) Sjögren 症候群 (SS) と EBV

SS と EBV との関連につき，Fox 等は EBV 早期抗原：EBV- encoded early antigen (EA-D) に対するモノクローナル抗体を用いて，SS 患者の唾液腺組織免疫組織染色をおこなうと 57%に EA-D を検出し，サザンブロット法にて耳下腺組織から EBVDNA を検出したことを報告している[25]．また Saito 等は PCR 法によって SS 患者末梢血，唾液腺組織でのウイルスコピー数の上昇を報告した[26]．

EBV は終生 B 細胞に潜伏感染するが，潜伏ウイルスがウイルス複製増殖を開始 (溶解感染) することをウイルスの再活性化といい，*in vitro* での研究により，再活性化には EBV 前早期遺伝子 BZLF1 および BRLF1 の発現により開始され，両者は協調し EBV 前早期遺伝子の発現を誘導する[27] ことが判明している．BZLF1 遺伝子産物である ZEBRA (Zta, EBI, Z protein) は複製にむけ最初に転写され，再活性化の指標となりうる重要な因子である．また SS における自己抗体の対応抗原が 120kD α-フォドリンであることが明らかにされ[28]，Saito 等は SS 患者の唾液腺組織で EBV 再活性化の際の ZEBRA 抗原の発現に伴い 120kD α-フォドリンの発現が誘導されることを明らかにした[29]．

(3) 血管炎と EBV

EBV はヘルペスウイルスγ亜科に分類され，霊長類でも種により EBV 類似γヘルペスウイルスの潜伏感染を受けている．動物モデルの研究において，Weck 等はマウスγヘルペスウイルス (γHV68) をインターフェロンγレセプター欠損マウスに感染させたところ，重篤な大血管の血管炎をおこし感染後14週までに死亡したと報告した[30]．

ヒトの血管炎症候群は侵される血管の太さによって分類され，大血管の血管炎は巨細胞血管炎 (側頭動脈炎) と高安動脈炎がそれにあたる．成人において EBV がこれらの疾患で検出された報告はないが，Kikuta 等は，慢性活動性 EBV 感染症の小児が川崎病類似の冠動脈の拡張所見を持ち，末梢血 EBNA 陽性リンパ球がすべて CD4+T 細胞であることを証明しており[31]，Nakagawa 等も小児の慢性活動性 EBV 感染症で冠動脈瘤と大動脈瘤血管病変の浸潤 T 細胞が EBER-1 陽性であることを報告している[32]．

3. 成人 T 細胞白血病ウイルス：HTLV-1

RA, SS と HTLV-1

HTLV-1 はレトロウイルスの一つであり，日本の西南部およびカリブ海地域に多発する成人 T 細胞白血病や HTLV-1 関連脊髄症 (HAM) の原因ウイルスとして知られている．HAM には RA 様多発関節炎の合併が見られその関連が検討されてきた．Eguchi 等は，HTLV-1 感染率の高い長崎市での検討により，HTLV-1 感染が RA と SS 発症の危険因子であることを疫学的に証明した[33]．*in vitro* の系において HTLV-1 感染 T 細胞と滑膜細胞を培養すると滑膜細胞に HTLV-1 が感染し，炎症性サイトカインが多量に産生され増殖する[34]．Iwakura 等によって HTLV-1 env-pX 領域を導入したトランスジェニックマウスでは，パンヌス形成や滑膜増殖が認められ RA 様の多発性関節炎が出現し，関節炎局所での炎症性サイトカインの産生増加発現，MHC クラス I, II の発現増強，II 型コラーゲン熱ショック蛋白に対する自己抗体産生や T 細胞の反応性の増強が見られた[35]．

Terada 等は，SS 患者唾液中の抗 HTLV-1 抗体陽性を測定したところ，IgA クラスの抗 HTLV-1 抗体が抗 HTLV-1 抗体陽性の SS 患者で高率に検出され，唾液腺局所での HTLV-1 に対する免疫応答の存在が示唆された[36]．

4. 内在性レトロウイルス

内在性レトロウイルス (human endogenous retrovirus: HERV) は，もともとは感染性レトロウイルスであったものが，進化の過程で宿主胚細胞ゲノムに組み込まれ子孫へと受け渡される遺伝子群であり，一部のものは転移性遺伝要素 (transposable genetic element：トランスポゾン) が進化したものとも考えられている．Yoshiki 等はヒト SLE のモデルマウスの NZB × NZWF1 では，肝での ERV が大量に発現され，gp 70 に対する抗体産生による免疫複合体の小血管炎や糸球体への沈着が報告され，内在性レトロウイルスが腎病変に関与することを示した[37]．混合性結合組織病 (MCTD) の自己抗原である U1 RNP の 70K 蛋白は，C 型レトロウイルス (レトロウイルスは電顕上の形態から A, B, C, D に分類される) の p30 gag 蛋白と相同性を持ち cross-reactivity を指摘されているが，Query 等はこの事実より HERV の gag 蛋白に対する抗体が，抗 U1 RNP 抗体の出現のトリガーとなるという説を唱えた[38]．また Human T-cell lymphotropic virus-related endogenous sequence (HRES)-1 に対しての抗体が U1 RNP の 70K 蛋白に交差反応を示し，HRES-1/p28 に対する抗体は SLE と重複症候群の 21～50%に検出される[39]．脱メチル化剤である 5-Azacytidine (5-AZA) がマウスにおいては HERV-E RNAC 型 ERV レトロウイルスに発現を増強することが報告されており，ヒトの正常リンパ球においては HERV-E RNA 発現を増強する．5-AZA 処理により T 細胞の DNA のメチル化が低下すると LFA-1 の発現が増強され自己反応性が亢進している[40]．また SLE 患者 T 細胞では DNA のメチル化低下が報告されており[41]，この異常が HERV の発現亢進に関与し，免疫異常が生じる可能性がある．

おわりに

以上，ウイルスとリウマチ性疾患・自己免疫疾患との関わりにつき述べてきた．近年，分子生物学的手法の急速な進歩とヒトゲノム解析により，疾患におけるウイルスの関わりは，病変部位におけるその存在証明だけでなく免疫学的・遺伝学的な病因への関与の解明を可能にしてきている．しかしモデル動物と異なり，遺伝的多様性を背景に持つヒトリウマチ性疾患・自己免疫疾患への環境因子あるいは遺伝的因子そのものとしてウイルスの病因への役割は今後更なる検討を要する．

文　献

1) Stieglitz A, Lipsky P. Association between reactive arthritis and antecedent infection with Shigella flexneri carrying a 2-Md plasmid and encoding an HLA-B27 mimetic epitope. *Arthritis Rheum* 1993; **36**: 1387–1391.
2) Xu XN, Screaton GR, McMichael AJ. Virus infections: escape, resistance, and counterattack. *Immunity* 2001; **15**: 867–870.
3) York IA, Roop C, Andrews DW, et al. A cytosolic herpes simplex virus protein inhibits antigen presentation to CD8+ T lymphocytes. *Cell* 1994; **77**: 525–535.
4) Geleziunas R, Xu W, Takeda K, Ichijo H, et al. HIV-1 Nef inhibits ASK1-dependent death signalling providing a potential mechanism for protecting the infected host cell. *Nature* 2001; 834–838.
5) Thome M, Schneider P, Hofmann K, et al. Viral FLICE-inhibitory proteins (FLIPs) prevent apoptosis induced by death receptors. *Nature* 1997; **386**: 517–521.
6) Mueller YM, De Rosa SC, Hutton JA, et al. Increased CD95/

Fas-induced apoptosis of HIV-specific CD8(+) T cells. *Immunity* 2001; **15**: 871–882.
7) Sandra T, Marialisa E, and Fernanda F. Human parvouirus B19 infection: Its relationship with systemic lupus erythematosus. *Seminars in Arthritis and Rheumatism* 1995; **28**: 319–325.
8) Pouchot J, Ouakil H, Debin ML, et al. Adult Still's disease associated with acute human parvovirus B19 infection. *Lancet* 1993; **341**: 1280–1281.
9) Chevrel G, Calvet A, Belin V, et al. Dermatomyositis associated with the presence of parvovirus B19 DNA in muscle. Rheumatology (Oxford) 2000; **39**: 1037–1039.
10) Ferri C, Zakrzewska K, Longombardo G, et al. Parvovirus B19 infection of bone marrow in systemic sclerosis patients. *Clin Exp Rheumatol* 1999; **17**: 718–720.
11) Boruchoff SE, Woda BA, Pihan GA, et al. Parvovirus B19-associated hemophagocytic syndrome. *Arch Intern Med* 1990; **150**: 897–899.
12) Murai C, Munakata Y, Takahashi Yet al. Rheumatoid arthritis after human parvovirus B19 infection. *Ann Rheum Dis* 1999; **58**: 130–132.
13) Takahashi Y, Murai C, Shibata S, et al. Human parvovirus B19 as a causative agent for rheumatoid arthritis. *Proc Natl Acad Sci USA* 1998; **95**: 8227–8232.
14) Moffatt S, Yaegashi N, Tada K, et al. Human parvovirus B19 nonstructural (NS1) protein induces apoptosis in erythroid lineage cells. *J Virol* 1998; **72**: 3018–3028.
15) Brown KE, Anderson SM, Young NS. Erythrocyte P antigen cellular receptor for B19 parvovirus. *Science* 1993; **262**: 114–117.
16) Alspaugh MA, Jensen FC, Rabin H, et al. Lymphocyte transformed by Epstein-Barr virus: induction of nuclear antigen reactive with antibody in rheumatoid arthritis. *J Exp Med* 1978; **147**: 1018–1027.
17) Rumpold H, Rhodes GH, Bloch PL, et al. The glycine-alanine repeating region is the major epitope of the Epstein-Barr nuclear antigen-1 (EBNA-1). *J Immunol* 1987; **138**: 593–599.
18) Fox R, Sportsman R, Rhodes G, et al. Rheumatoid arthritis synovial membrane contains a 62000-molecular-weight protein that shares an antigenic epitope with the Epstein Barr virus encoded associated nuclear antigen. *J Clin Inv* 1986; **77**: 1539–1547.
19) Takei M, Mitamura K, Fujiwara N, et al. Detection of Epstein-Barr virus-encoded small RNA 1 and latent membrane protein 1 in synovial lining cells from rheumatoid arthritis patients. *Int Immunol* 1997; **9**: 739–743.
20) Takeda T, Mizugaki Y, Matsubara L, et al. Lytic Epstein-Barr virus infection in the synovial tissue of patients with rheumatoid arthritis. *Arthritis Rheum* 2000; **43**: 1218–1225.
21) Hirohata S, Yanagida T, Nakamura H, et al. Bone marrow CD34+ progenitor cells from rheumatoid arthritis patients support spontaneous transformation of peripheral blood B cells from healthy individuals. *Rheum Int* 20001; **9**: 153–159.
22) Blaschke S, Schwarz G, Moneke D, et al. Epstein-Barr virus infection in peripheral blood mononuclear cells, synovial fluid cells, and synovial membranes of patients with rheumatoid arthritis. *J Rheumatol* 2000; **27**: 866–873.
23) Sayos J, Wu C, Morra M, et al. The X-linked lymphoproliferative-disease gene product SAP regulates signals induced through the co-receptor SLAM. *Nature* 1998; **395**: 462–469.
24) Takei M, Ishiwata T, Mitamura K, et al. Decreased expression of signaling lymphocytic-activation molecule associated protein (SAP) transcripts in T cells from patients with rheumatoid arthritis. *Int Immunol* 2001; **13**: 559–565.
25) Fox RI, Pearson G, Vaughan JH. Detection of Epstein-Barr virus-associated antigens and DNA in salivary gland biopsies from patients with Sjogren's syndrome. *J Immunol* 1986; **137**: 3162–3168.
26) Saito I, Servenius B, Compton T, Fox RI. Detection of Epstein-Barr virus DNA by polymerase chain reaction in blood and tissue biopsies from patients with Sjogren's syndrome. *J Exp Med* 1989; **169**: 2191–2198.
27) Chevallier-Greco A, Manet E, Chavrier P, et al. Both Epstein-Barr virus (EBV)-encoded trans-acting factors, EB1 and EB2, are required to activate transcription from an EBV early promoter. *EMBO J* 1986; **5**: 3243–3249.
28) Haneji N, Nakamura T, Takio K, et al. Identification of alpha-fodrin as a candidate autoantigen in primary Sjogren's syndrome. *Science* 1997; **25**: 604–607 .
29) Inoue H, Tsubota K, Ono M, et al. Possible involvement of EBV-mediated alpha-fodrin cleavage for organ-specific autoantigen in Sjogren's syndrome. *J Immunol* 2001; **166**: 5801–5809.
30) Weck KE, Dal Canto AJ, Gould JD, et al. Murine gamma-herpesvirus 68 causes severe large-vessel arteritis in mice lacking interferon-gamma responsiveness: a new model for virus-induced vascular disease. *Nat Med* 1997; **3**: 1346–1353.
31) Kikuta H, Taguchi Y, Tomizawa K, et al. Epstein-Barr virus genome-positive T lymphocytes in a boy with chronic active EBV infection associated with Kawasaki-like disease. *Nature* 1988; **333**: 455–457.
32) Nakagawa A, Ito M, Iwaki T, Yatabe Y, et al. Chronic active Epstein-Barr virus infection with giant coronary aneurysms. *Am J Clin Pathol* 1996; **105**: 733–736.
33) Eguchi K, Origuchi T, Takashima H, et al. High seroprevalence of anti-HTLV-I antibody in rheumatoid arthritis. *Arthritis Rheum* 1996; **39**: 463–466.
34) Sakai M, Eguchi K, Terada K, et al. Infection of human synovial cells by human T cell lymphotropic virus type I. Proliferation and granulocyte/macrophage colony-stimulating factor production by synovial cells. *J Clin Invest* 1993; **92**: 1957–1966.
35) Iwakura Y, Tosu M, Yoshida E, et al. Induction of inflammatory arthropathy resembling rheumatoid arthritis in mice transgenic for HTLV-I. *Science* 1991; **253**: 1026–1028.
36) Terada K, Katamine S, Eguchi K, et al. Prevalence of serum and salivary antibodies to HTLV-1 in Sjogren's syndrome. *Lancet* 1994; **344**: 1116–1119.
37) Yoshiki T, Mellors RC, Strand M, et al. The viral envelope glycoprotein of murine leukemia virus and the pathogenesis of immune complex glomerulonephritis of New Zealand mice. *J Exp Med* 1974; **140**: 1011–1027.
38) Query CC, Keene JD. A human autoimmune protein associated with U1 RNA contains a region of homology that is cross-reactive with retroviral p30gag antigen. *Cell* 1987; **51**: 211–220.
39) Perl A, Colombo E, Dai H, et al. Antibody reactivity to the HRES-1 endogenous retroviral element identifies a subset of patients with systemic lupus erythematosus and overlap syndromes. Correlation with antinuclear antibodies and HLA class II alleles. *Arthritis Rheum* 1995; **38**: 1660–1671.
40) Richardson BC, Strahler JR, Pivirotto TS, et al. Phenotypic and functional similarities between 5-azacytidine-treated T cells and a T cell subset in patients with active systemic lupus erythematosus. *Arthritis Rheum* 1992; **35**: 647–662.
41) Richardson B, Scheinbart L, Strahler J, et al. Evidence for impaired T cell DNA methylation in systemic lupus erythematosus and rheumatoid arthritis. *Arthritis Rheum* 1990; **33**: 1665–1673.

Reactivation of Immanent Herpes Group Virus

Shigemasa SAWADA, MD and Masami TAKEI, MD

Reprinted from Internal Medicine
Vol. 42, No. 2, Pages 140–141
February 2003

□ EDITORIAL □

Reactivation of Immanent Herpes Group Virus

Key words: herpes virus, Epstein-Barr virus, drug induced skin rash, herpes zoster rheumatoid arthritis, hypersensitivity syndrome

Recent modern molecular biology techniques indicate the involvement of herpes viruses in the pathogenesis of some diseases. Herpes group viruses include cytomegalovirus, Epstein-Barr virus (EBV), herpes simplex 1 or 2, varicella zoster virus, human herpes virus (HHV)-6, HHV-7 and HHV-8. These viruses are transferred by human contact and cause a primary infection, which commonly does not show clinical signs and may exist even for years in a latent state in healthy individuals by means of suppressive immune regulation. Nonetheless, those viruses may be reactivated by the dysregulation of the host immune system or possibly by virus mutations. There is a great deal of evidence of the association of herpes simplex virus and recurrent erythema multiforme. This association has been supported by clinical and laboratory studies. Huff and Weston indicated that patients had a history of herpes simplex virus infection proceeding their as analyzed episode and their sera had antibodies to this virus by enzyme immunoassay (1). Furthermore, they demonstrated that herpes simplex virus antigen was detected in the skin biopsy specimens by an indirect immunofluorescent technique with a monoclonal antibody to the type common human simplex virus glycoprotein gB around keratinocytes in the epidermis.

Brice et al demonstrated herpes simplex virus (HSV) DNA in the cutaneous lesions of erythma multiforme, by means of polymerase chain reaction and, by *in-situ* hybridization with ^{35}S-labeled HSV-RNA probe within the epidermis (2). Many reports have discussed the role of viral infection and drug induced skin rash, and showed clinical evidence that cutaneous rashes are observed in more than 90% of patients given ampicillin in patients with infectious mononucleosis whereas usually are observed in less than 15% in patients without it (3) and that an extraordinary high incidence of Stevens-Johnson syndrome in patients infected with human immunodeficiency virus (4).

Kunishige et al (5) in this journal described that Salazosulfapirigine induced hypersensitivity syndrome associated with reactivation of human herpes virus 6.

See also p 203.

A hypersensitivity syndrome has been reported with the administration of a limited number of drugs, such as allopurinol, dapsone, minocycline and phenytoin (6), suggesting that the specified structure of drug involves a hypersensitivity syndrome or a latent virus reactivation. Even though the precise mechanism by which viral infection causes the drug-associated skin rash remains unclear, it has been suggested that the regulatory gene mutation defines the reactivation of herpes simplex virus latency (7).

A reactivation of immanent virus may be a crucial event for the development of a severe drug-induced hypersensitivity syndrome.

The ampicillin rash appeared in patients only in primary EBV infection but not in the recovery period (3). This report suggested that skin rash may be incriminated by the EB virus reactivation. We have often observed herpes zoster or trigeminal nerve paralysis, which is thought to be reactivation of herpes simplex virus in patients with rheumatoid arthritis (RA). Indeed, it has been reported that there is an increased subsequent risk of RA in patients diagnosed with herpes zoster (8, 9).

Primary EB virus infection is characterized by atypical lymphocytes which are the CD8+ T cell subset. These CD8+ T cells play the role of MHC-restricted virus-specific cytotoxic T cell function. We examined the synovial tissues from 34 patients with RA and from 20 patients with osteoarthritis (OA), and from one patient with psoriatic arthritis as controls, for evidence of the EBV by *in-situ* hybridization. The specimens were also tested by immunoperoxidase staining for expression of EBV nuclear antigen (EBNA)-2 and latent membrane protein (LMP)-1. EBV-encoded small RNA-1 (EBER) was demonstrated in synovial lining cells from eight (23.5%) out of 34 RA patients but in none of 20 OA patients ($p<0.05$) nor in the one psoriatic arthritis patient. Furthermore, LMP-1 was also detected in synovial lining cells. Nevertheless, EBNA-2 was not demonstrated in such lesions. The incidence of EBV existence in synovial lining cells with severely infiltrated lymphocytes tended to be higher than that in moderately infiltrated ones (10).

In a recent study searching for the causative gene of X-linked lymphoproliferative syndrome, the gene linked to EBV-specific cytotoxic T cells or NK cell-mediated cytotoxic activity to EBV-infected cells was discovered, and its product is now referred to as signaling lymphocytic-activation molecule-associated protein (SAP) or Src homology 2 domain-containing protein (SH2D1A) (11). We have found that the expression level of SAP transcripts in peripheral leukocytes of RA patients was significantly lower than that of normal individuals ($p=0.0007$), that of inactive syste-

mic lupus erythematosus or that of chronic renal diseases. There was no mutation in the coding region of SAP cDNAs derived from peripheral leukocytes of RA patients. The decreased expression of SAP transcripts in peripheral leukocytes or T cells of RA patients might lead to the failure of the immune system to eliminate the EBV-infected synovial lining cells in joints of RA patients (12).

Taken together, the reactivation of latent virus might be due to the mutation of latent virus or due to the decreased regulatory function of human genes for the drug-induced rash.

Shigemasa SAWADA, MD*·** and Masami TAKEI, MD**
*Department of Medicine, Nerima Hikarigaoka Nihon University Hospital, 2-11-1 Hikarigaoka, Nerima-ku, Tokyo 179-0072
and **Department of Medicine, 1st Department of Medicine, Nihon University School of Medicine, 30 Kamimachi, Ohyaguchi, Itabashi-ku, Tokyo 173-8610

References

1) Huff JC, Weston WL. Recurrent erythema multiforme. Medicine (Baltimore) **68**: 133–140, 1989.
2) Brice SL, Krezemien D, Weston WL, Huff JC. Detection of herpes simplex virus DNA in cutaneous lesions of erythema multiforme. J Invest Dermatol **93**: 183–187, 1989.
3) Pullen H, Wright N, Murdoch JM. Hypersensitivity reactions to antibacterial drugs in infectious mononucleosis. Lancet **2**: 1176–1178, 1967.
4) Rzany B, Mockenhaupt M, Stocker U, Hamouda O, Schopf E. Incidence of Stevens-Johnson syndrome and toxic epidermal necrolysis in patients with the acquired immunodeficiency syndrome in Germany. Arch Dermatol **129**: 1059, 1993 (letter).
5) Kunisaki Y, Goto H, Kitagawa K, Nagano M. Salazosulfapyridine induced hypersensitivity syndrome associated with reactivation of humanherpes virus 6. Intern Med **42**: 203–207, 2003.
6) Mizukawa Y, Shiohara T. Virus-induced immune dysregulation as a triggering factor for the development of drug rashes and autoimmune diseases: with emphasis on EB virus, human virus 6 and hepatitis C virus. J Dermatol Sci **22**: 169–180, 2000.
7) Leib DA, Coen DM, Bogard CL, Hicks KA, Yager DR, Knipe DM. Immediate-early regulatory gene mutants define different stages in the establishment and reactivation of herpes simplex virus latency. J Virol **63**: 759–768, 1989.
8) Ragozzino MW, Kurland LT. Subsequent risk of rheumatoid arthritis in patients diagnosed with herpes zoster. Lancet 16; **2** (8303): 884, 1982 (letter).
9) Campalani E, Meenagh GK, Finch MB. Case Number 22: An interesting case of herpes zoster in rheumatoid arthritis. Ann Rheum Dis **61**: 102, 2002.
10) Takei M, Mitamura K, Fujiwara S, et al. Detection of Epstein-Barr virus-encoded small RNA 1 and latent membrane protein 1 in synovial lining cells from rheumatoid arthritis patients. Int Immunol **9**: 739–743, 1997.
11) Sayos J, Wu C, Morra M, et al. The X-linked lymphoproliferative-disease gene product SAP regulates signals induced through the co-receptor SLAM. Nature 1; **395** (6701): 462–469, 1998.
12) Takei M, Ishiwata T, Mitamura K, et al. Decreased expression of signaling lymphocytic-activation molecule-associated protein (SAP) transcripts in T cells from patients with rheumatoid arthritis. Int Immunol **13**: 559–565, 2001.

SgIGSF: a new mast-cell adhesion molecule used for attachment to fibroblasts and transcriptionally regulated by MITF

Akihiko Ito, Tomoko Jippo, Tomohiko Wakayama, Eiichi Morii, Yu-ichiro Koma, Hiroaki Onda, Hiroshi Nojima, Sholchi Iseki, and Yukihiko Kitamura

Microphthalmia transcription factor (MITF) is a basic-helix-loop-helix-leucine zipper-type transcription factor. The mutant *mi* and *Mi^{wh}* alleles encode MITFs with deletion and alteration of a single amino acid, respectively, whereas the *tg* is a null mutation. In coculture with NIH/3T3 fibroblasts, the numbers of cultured mast cells (CMCs) derived from C57BL/6 (B6)$^{mi/mi}$, B6$^{Miwh/Miwh}$, and B6$^{tg/tg}$ mice that adhered to NIH/3T3 fibroblasts were one third as large as the number of B6$^{+/+}$ CMCs that adhered to NIH/3T3 fibroblasts. From a cDNA library of B6$^{+/+}$ CMCs, we subtracted messenger RNAs expressed by B6$^{mi/mi}$ CMCs and found a clone encoding SgIGSF, a recently identified member of the immunoglobulin superfamily. Northern and Western blot analyses revealed that SgIGSF was expressed in B6$^{+/+}$ CMCs but not in CMCs derived from MITF mutants. Immunocytochemical analysis showed that SgIGSF localized to the cell-to-cell contact areas between B6$^{+/+}$ CMCs and NIH/3T3 fibroblasts. Transfection of B6$^{mi/mi}$ and B6$^{tg/tg}$ CMCs with SgIGSF cDNA normalized their adhesion to NIH/3T3 fibroblasts. NIH/3T3 fibroblasts did not express SgIGSF, indicating that SgIGSF acts as a heterophilic adhesion molecule. Transfection of B6$^{tg/tg}$ CMCs with normal MITF cDNA elevated their SgIGSF expression to normal levels. These results indicated that SgIGSF mediated the adhesion of CMCs to fibroblasts and that the transcription of SgIGSF was critically regulated by MITF. (Blood. 2003;101:2601-2608)

Introduction

The mouse *mi* locus encodes a transcription factor belonging to the basic-helix-loop-helix-leucine zipper family denoted hereafter as the microphthalmia transcription factor (MITF).[1,2] The mutant *mi* allele produces an abnormal MITF protein that lacks 1 of the 4 consecutive arginines in the basic domain (denoted hereafter as *mi*-MITF).[1,3,4] The *mi*-MITF is defective in DNA binding, nuclear translocation, and transactivation of target genes.[5-8] Another mutant allele is the *tg* allele, which is the MITF gene bearing a transgene insertion mutation in its 5′ flanking region.[1,9] Although the coding region of the MITF gene in C57BL/6 (B6)$^{tg/tg}$ mice is normal, significant amounts of MITF were not detectable in cultured mast cells (CMCs) derived from the spleens of B6$^{tg/tg}$ mice.[10]

Both B6$^{mi/mi}$ and B6$^{tg/tg}$ mice show microphthalmia, lack of melanocytes, and a decrease in skin mast cells.[11] B6$^{mi/mi}$ mice show osteopetrosis but B6$^{tg/tg}$ mice do not.[12] Most B6$^{mi/mi}$ mice die upon weaning due to the failure of tooth eruption caused by the osteopetrosis, whereas most B6$^{tg/tg}$ mice survive to adulthood. Mast cell numbers in skin tissues were comparable between B6$^{mi/mi}$ and B6$^{tg/tg}$ mice.[13] However, only B6$^{mi/mi}$ mice showed a decrease of heparin content in skin mast cells.[14]

Gene expression profiles of CMCs were compared between B6$^{mi/mi}$ and B6$^{tg/tg}$ mice. The transcription of mouse mast cell protease 2 (mMCP-2), mMCP-4, mMCP-5, mMCP-6, and mMCP-9 genes decreased severely in both B6$^{mi/mi}$ CMCs and B6$^{tg/tg}$ CMCs.[15-18] The transcription of the genes encoding c-*kit* receptor tyrosine kinase (KIT), granzyme B, tryptophan hydroxylase, and N-deacetylase/N-sulfotransferase 2 was reduced severely in B6$^{mi/mi}$ CMCs, but the reduction of transcription of these genes was not so severe in B6$^{tg/tg}$ CMCs.[8,13,19] This indicated that the *mi*-MITF possessed an inhibitory effect on the transcription of KIT,[19] granzyme B, tryptophan hydroxylase, and N-deacetylase/N-sulfotransferase 2 genes.[8,13,19]

We have shown that B6$^{mi/mi}$ CMCs have a variety of abnormal phenotypes.[5-8] One is that they adhere poorly to fibroblasts.[20] A considerable number of B6$^{+/+}$ CMCs cultured on a monolayer of fibroblasts adhere to the fibroblasts,[20-22] but significantly fewer B6$^{mi/mi}$ CMCs do this.[20] In the present study, we examined the number of B6$^{tg/tg}$ CMCs that adhered to NIH/3T3 fibroblasts. We also assessed the adherence to fibroblasts of CMCs derived from B6$^{Miwh/Miwh}$ mice, which have a single altered amino acid in the basic domain of MITF.[23] We found that B6$^{tg/tg}$ and B6$^{Miwh/Miwh}$ CMCs were as poor as B6$^{mi/mi}$ CMCs in adhering to fibroblasts. From a cDNA library of B6$^{+/+}$ CMCs, we subtracted messenger RNAs expressed by B6$^{mi/mi}$ CMCs. By screening the subtracted cDNA library, we identified a new mast cell adhesion molecule, SgIGSF (spermatogenic immunoglobulin superfamily),[24] whose transcription was critically regulated by normal MITF (+-MITF) in CMCs. The deficient transcription of SgIGSF appeared to be a cause of the defective adhesion of CMCs derived from MITF mutant mice to NIH/3T3 fibroblasts.

From the Department of Pathology, Osaka University Medical School/Graduate School of Frontier Bioscience, Suita, Osaka; the Department of Histology and Embryology, Graduate School of Medical Science, Kanazawa University, Kanazawa, Ishikawa; and the Department of Molecular Genetics, Institute for Microbial Diseases, Osaka University, Suita, Osaka, Japan.

Submitted July 29, 2002; accepted November 19, 2002. Prepublished online as *Blood* First Edition Paper, November 27, 2002; DOI 10.1182/blood-2002-07-2265.

Supported by grants from the Ministry of Education, Culture, Sports, Science and Technology; the Osaka Cancer Society; the Sagawa Foundation for Promotion of Cancer Research; and the Naito Foundation.

Reprints: Yukihiko Kitamura, Department of Pathology, Osaka University Medical School, 2-2 Yamada-oka, Suita, Osaka 565-0871, Japan; e-mail: kitamura@patho.med.osaka-u.ac.jp.

The publication costs of this article were defrayed in part by page charge payment. Therefore, and solely to indicate this fact, this article is hereby marked "advertisement" in accordance with 18 U.S.C. section 1734.

Materials and methods

Mice

The original stock of $B6^{mi/+}$ and $B6^{Mlwbl/+}$ mice was purchased from the Jackson Laboratory (Bar Harbor, ME). VGA-$9^{tg/tg}$ mice were kindly provided by Dr H. Arnheiter (National Institutes of Health, Bethesda, MD). All MITF mutant mice were maintained by consecutive back-crosses to our own inbred B6 colony (more than 12 generations at the time of the present experiment). Homozygous mice were produced by crosses between female and male heterozygotes of each genotype and selected by their white coat color. The $WB^{+/+}$, $WB^{W/W}$, $WBB6F_1^{+/+}$, and $WBB6F_1^{W/W}$ mice were purchased from Japan SLC (Hamamatsu, Japan).

Cells

Spleens from 2- to 3-week-old mice were first passed through a 23-gauge needle and then cultured in α–minimal essential medium (α-MEM; ICN Biomedicals, Costa Mesa, CA) supplemented with 10% pokeweed mitogen-stimulated spleen cell–conditioned medium (PWM-SCM) and 10% fetal calf serum (FCS; Nippon Biosupply Center, Tokyo, Japan). PWM-SCM was prepared as described previously.[25] Half of the medium was replaced every 7 days. Four weeks later, more than 95% of the cells were CMCs. To examine growth kinetics of CMCs, 2.5×10^5 CMCs were suspended in 2 mL α-MEM supplemented with 10% PWM-SCM and 10% FCS and plated onto 35-mm culture dishes. Various days after the plating, total cell numbers were counted with a standard hemocytometer. MST mastocytoma cells[26] were kindly provided by Dr J. D. Esko (University of California, San Diego, CA). Ψ2 helper virus–free packaging cells, NIH/3T3 mouse fibroblastic cells, and Jurkat lymphoid cells were maintained as described previously.[19,27,28]

Coculture of CMCs with fibroblasts and evaluation of attachment

Coculture of CMCs with NIH/3T3 cells was performed as described previously.[21,22] Briefly, CMCs (1.0×10^5 cells per dish) were suspended in 2 mL α-MEM containing 10% FCS and added to a confluent culture of NIH/3T3 cells in 35-mm culture dishes. In some experiments, PWM-SCM was added to a concentration of 10%. After 3 hours of coculture, the dishes were washed with warmed (37°C) α-MEM to remove nonadherent CMCs. NIH/3T3 cells and adherent CMCs were harvested by trypsin treatment. These cells were attached to microscope slides using the Cytospin 2 centrifuge (Shandon, Pittsburgh, PA), fixed with Carnoy solution, and stained with alcian blue and nuclear fast red. The proportion of alcian blue–positive mast cells to alcian blue–negative NIH/3T3 cells was determined. Each experiment was done in triplicate and repeated 3 times with similar results.

cDNA libraries and isolation of clones

A cDNA library of $B6^{+/+}$ CMCs and the (*+/+ − mi/mi*) subtracted cDNA library were constructed previously.[7,29] Sequencing and isolation of clones from the libraries were performed as described previously.[7,27] The DNA sequences were used to search the National Center for Biotechnology Information database using the BLASTN algorithm.

Northern blotting and hybridization was performed using standard methods. Relative signal intensity was calculated with the BAS 2000 system (Fuji Photo Film, Tokyo, Japan). cDNA inserts of clones from the libraries and the β-actin cDNA fragment[7] were labeled with α-^{32}P dCTP by the random labeling method.

Antibodies

A rabbit polyclonal antibody against SgIGSF was made in Kanazawa University (by T.W. and S.I.). The method of preparation and the sensitivity of the antibody are described in detail elsewhere (T.W. and S.I., manuscript submitted, 2002). Briefly, rabbits were immunized against the synthetic polypeptide containing 15 amino acids of the C-terminus of SgIGSF. Four months later, the rabbit sera were purified with an affinity column containing the synthetic polypeptide. The anti-MITF antibody has been described previously.[30] Other primary antibodies used were specific for KIT (M-14; Santa Cruz Biotechnology, Santa Cruz, CA), E-cadherin (Clone 36; Transduction Laboratories, Lexington, KY), N-cadherin (Clone 32; Transduction Laboratories), ICAM-1 (KAT-1; Seikagaku, Tokyo, Japan), integrin β3 (Transduction Laboratories), and α-tubulin (DM 1A; Sigma Chemical, St Louis, MO). Secondary antibodies used were peroxidase-labeled antirabbit, antimouse, or antirat immunoglobulin G (IgG) antibodies (MBL, Nagoya, Japan), and fluorescein isothiocyanate (FITC)–labeled antirabbit IgG antibody (MBL).

Western blot analysis

CMCs and mouse tissues were lysed in a buffer containing 50 mM Tris-HCl (pH 8.0), 150 mM NaCl, 1% Triton X-100, and 1 mM phenylmethylsulfonyl fluoride. The resulting lysates were separated on 10% sodium dodecyl sulfate (SDS)–polyacrylamide gels, transferred to Immobilon (Millipore, Bedford, MA), and reacted with the primary antibodies indicated. After washing, the blots were incubated with an appropriate peroxidase-labeled secondary antibody and then reacted with Renaissance reagents (NEN, Boston, MA) before exposure. After stripping, the blots were probed with the anti–α-tubulin antibody.

Enzymatic digestion of N-linked glycosylation

A 20-μL volume of CMC pellet was denatured at 100°C for 10 minutes and then one tenth of the sample was incubated at 37°C for 1 hour in the presence or absence of Peptide:*N*-glycocidase F (PNGase F; 500 U) according to kit instructions (New England Biolabs, Beverly, MA). The samples were then separated on SDS-polyacrylamide gels and reacted with the anti-SgIGSF antibody.

Transfection of CMCs with retroviral vector

The pCX4bsr vector, a modified pCXbsr vector,[31] was kindly provided by Dr T. Akagi (Osaka Bioscience Institute, Osaka, Japan). A clone containing full-length SgIGSF cDNA was isolated from the $B6^{+/+}$ CMC cDNA library. The cDNA insert was excised by *Eco*RI digestion and inserted directionally into the pCX4bsr retroviral vector via the *Eco*RI site. The resulting pCX4bsr-SgIGSF vector or the empty pCX4bsr vector was then transfected into the packaging cell line Ψ2, and blasticidin-resistant Ψ2 cell clones were selected by culturing in α-MEM containing 10% FCS and blasticidin (3μg/mL; Invitrogen, Carlsbad, CA). To obtain infected CMCs, a subconfluent monolayer of the Ψ2 cell clones that produce high titers of retrovirus containing either the SgIGSF cDNA or no insert was γ-irradiated at a single dose of 30 Gy. A freshly prepared spleen cell suspension was then added to the monolayer and incubated for 5 days in α-MEM containing 10% FCS and 10% PWM-SCM. Blasticidin-resistant CMCs were selected by continuing the culture in the presence of blasticidin (1.5 μg/mL) for 4 weeks. Transfection of CMCs with a retrovirus vector containing the +-MITF cDNA was performed as described previously.[19]

NIH/3T3 cells were transfected with the pCX4bsr-SgIGSF vector by the calcium phosphate coprecipitation method. Blasticidin-resistant NIH/3T3 cells were selected by continuing the culture in the presence of blasticidin (3 μg/mL) for 4 weeks.

Immunocytochemistry

CMCs were washed with phosphate-buffered saline (PBS; pH 7.4), attached to microscope slides by Cytospin 2 centrifugation (Shandon), and fixed with methanol. For staining the coculture, an NIH/3T3 monolayer was established on a cover slip placed at the bottom of a culture dish and CMCs were plated over this. After 3 hours' coculture, the cover slips were washed with PBS and fixed with methanol. Fixed samples were blocked with 2% bovine serum albumin in PBS, incubated with the anti-SgIGSF antibody, and stained with FITC-labeled antirabbit IgG antibody. For double staining with phalloidin, the coculture samples were fixed with 3.7% paraformaldehyde in PBS and permeabilized with 0.1% Triton X-100 in PBS. After staining with the anti-SgIGSF antibody as described above, the samples were

Table 1. Poor attachment of B6$^{mi/mi}$, B6$^{tg/tg}$, and B6 Mi^{wh}/Mi^{wh} CMCs to NIH/3T3 fibroblasts

CMC genotype	No. of adhering CMCs per NIH/3T3 cell*	
	PWM-SCM⁻†	PWM-SCM⁺†
+/+	0.166 ± 0.021	0.162 ± 0.028
mi/mi	0.042 ± 0.017‡	0.044 ± 0.022‡
tg/tg	0.044 ± 0.010‡	0.048 ± 0.023‡
Mi^{wh}/Mi^{wh}	0.040 ± 0.011‡	0.046 ± 0.012‡

*Mean ± SE of 3 dishes.

†The coculture of CMCs and NIH/3T3 cells was done with (+) or without (−) PWM-SCM (10%).

‡$P < .01$ by Student t test when compared with the values of B6$^{+/+}$ CMCs.

incubated with tetramethylrhodamine isothiocyanate (TRITC)–labeled phalloidin (1:5,000 dilution; Sigma). Cells were visualized using a confocal laser scanning microscope (LSM510; Carl Zeiss, OberKochen, Germany).

Luciferase assay

The pEF-BOS vectors[32] containing +-MITF or *mi*-MITF cDNA, constructed previously,[19] were used as effectors. The 5′ flanking sequence of the SgIGSF gene was obtained from the database of the Celera Discovery System (Celera, Rockville, MD). The genomic region of nucleotide (nt) −1501 to +19 of the SgIGSF gene was amplified by PCR and subcloned into the upstream region of the luciferase gene in pSPLuc plasmid. A reporter and an effector were electroporated together into MST mastocytoma and Jurkat lymphoid cells as described previously.[13,27] The relative luciferase activity was calculated as described previously.[7]

Electrophoretic gel mobility shift assay (EGMSA)

Glutathione S-transferase (GST) and GST–+-MITF were produced previously.[5] Two oligonucleotides were synthesized: E, 5′-GCTTTAATGTGTAACTCATTTGATGGGTTGGCCGA-3′ (nt −1506 to −1472 of the SgIGSF promoter), and mE, 5′-GCTTTAATGTGTAACTC*T*TTAGATGGGTTGGCCGA-3′. EGMSA was performed as described previously.[7]

Results

Poor attachment of CMCs derived from MITF mutants to NIH/3T3 fibroblasts

We examined numbers of B6$^{+/+}$, B6$^{mi/mi}$, B6$^{tg/tg}$, and B6$^{Miwh/Miwh}$ CMCs that adhered to NIH/3T3 cells 3 hours after the initiation of the coculture. The number of adhering B6$^{mi/mi}$, B6$^{tg/tg}$, or B6$^{Miwh/Miwh}$ CMCs was one third that of B6$^{+/+}$ CMCs (Table 1). No significant difference was observed among numbers of adhering B6$^{mi/mi}$, B6$^{tg/tg}$, and B6$^{Miwh/Miwh}$ CMCs. As we reported previously,[20] addition of PWM-SCM to the coculture did not affect the results (Table 1).

Isolation of SgIGSF gene as a transcriptionally down-regulated gene in B6$^{mi/mi}$ CMCs

We constructed a cDNA library from B6$^{+/+}$ CMCs and subtracted from it mRNAs expressed in B6$^{mi/mi}$ CMCs.[7] The (+/+ − *mi/mi*) subtracted cDNA library proved to be enriched with clones that were transcriptionally down-regulated in B6$^{mi/mi}$ CMCs.[7,8] From the subtracted library, we attempted to isolate cDNA clones whose gene product might explain the deficient adhesion of B6$^{mi/mi}$ and B6$^{tg/tg}$ CMCs to NIH/3T3 cells. We sequenced approximately 600 clones from the library and found a clone (no. 236) that carried part of the cDNA sequence encoding SgIGSF. The cDNA of SgIGSF was recently cloned from mouse testes, and it has a putative transmembrane domain and an extracellular domain consisting of 3 immunoglobulin-like loops.[24]

We performed Northern blot analysis on RNAs extracted from B6$^{+/+}$, B6$^{mi/mi}$, and B6$^{tg/tg}$ CMCs, using clone 236 as a probe. Two transcripts were detected near the positions of 28S and 18S in B6$^{+/+}$ CMCs: the expression of the longer transcript was much stronger than that of the shorter one (Figure 1A). This result was consistent with the result reported by Wakayama et al[24] that the SgIGSF gene has 2 transcripts of 4.5 and 2.1 kb in mouse testes. In contrast to the case of B6$^{+/+}$ CMCs, no hybridization signals were detected in RNAs obtained from either B6$^{mi/mi}$ or B6$^{tg/tg}$ CMCs (Figure 1A). We screened the original cDNA library of B6$^{+/+}$ CMCs by using clone 236 as a probe and isolated 5 positive clones carrying a cDNA insert of approximately 2.1 kb. Sequencing revealed that the cDNA inserts of all clones were identical to the reported full-length cDNA of the SgIGSF gene (accession no. AB052293).

Protein expression of SgIGSF was examined by blotting the lysates of CMCs from various genotypes with the anti-SgIGSF antibody (Figure 1B). Two strong bands of approximately 110 and 38 kDa and a weak band of approximately 50 kDa were observed in the B6$^{+/+}$ CMC lysate. In the lysates of B6$^{mi/mi}$, B6$^{tg/tg}$, and B6$^{Miwh/Miwh}$ CMCs, the bands of approximately 110 and 38 kDa were not detectable but the band of approximately 50 kDa was recognizable (Figure 1B).

Western blotting was also performed on the lysates of intact NIH/3T3 cells and NIH/3T3 cells that had been transfected with full-length SgIGSF cDNA. No band was observed in the lysate of intact NIH/3T3 cells. In the transfected NIH/3T3 cells, 4 bands were recognized, and the bands representing the longest and shortest proteins were positioned at mobility sizes similar to those of the 2 strong bands observed in B6$^{+/+}$ CMCs (Figure 1B). Thus, we considered that SgIGSF had 2 forms, of approximately 110 and

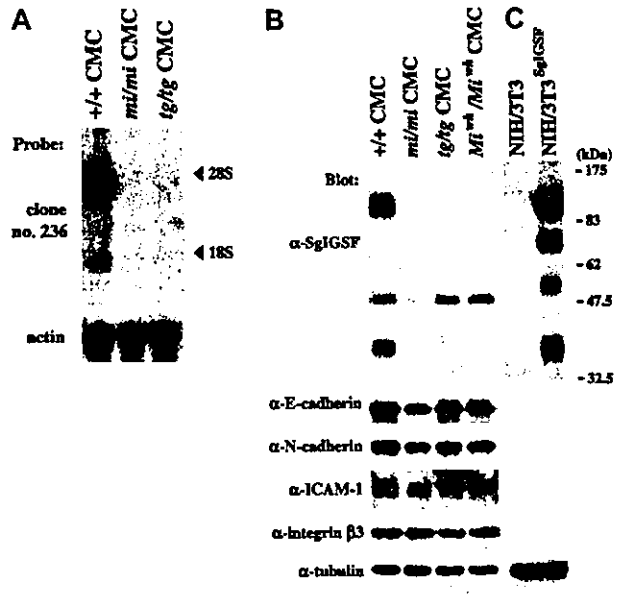

Figure 1. Expression of SgIGSF and intercellular adhesion molecules in CMCs derived from MITF mutant mice. (A) Expression of SgIGSF mRNA in B6$^{+/+}$, B6$^{mi/mi}$, and B6$^{tg/tg}$ CMCs. RNA (10 μg of total RNA) from CMCs of 3 genotypes was electrophoresed and hybridized with the clone 236 probe. After stripping, the blot was hybridized with the β-actin probe to indicate the amount of RNA loaded per lane. (B) Expression of the SgIGSF protein and intercellular adhesion molecules in B6$^{+/+}$, B6$^{mi/mi}$, B6$^{tg/tg}$, and B6$^{Miwh/Miwh}$ CMCs. Lysates of the indicated cells were electrophoresed and blotted with antibodies against SgIGSF, E-cadherin, N-cadherin, ICAM-1, and integrin β3. (C) Western blot analysis of NIH/3T3 cells and those transfected with SgIGSF cDNA (NIH/3T3^{SgIGSF}). The lysates of the indicated cells were electrophoresed and blotted with the SgIGSF antibody and then probed again with the anti-α-tubulin antibody to indicate the total amount of proteins loaded per lane. The molecular weight scale is shown to the right of the blot.

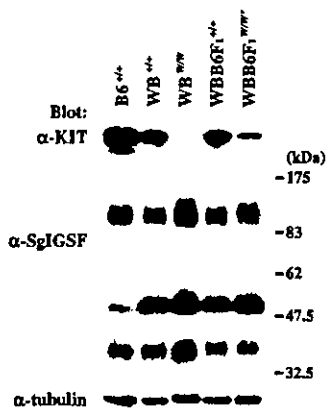

Figure 2. SgIGSF expression in CMCs derived from KIT mutant mice. Lysates were prepared from CMCs derived from mice of the indicated genotypes and were blotted with the anti-KIT and anti-SgIGSF antibodies. The molecular weight scale is shown to the right of the blots. The blots were probed again with the anti–α-tubulin antibody to indicate the total amount of proteins loaded per lane.

38 kDa, in B6$^{+/+}$ CMCs, but these forms were absent from B6$^{mi/mi}$, B6$^{tg/tg}$, and B6-*Mi^{wh}/Mi^{wh}* CMCs. A weak band of approximately 50 kDa detected in all 4 types of CMCs remained uncharacterized. Because there is no SgIGSF mRNA expression in B6$^{mi/mi}$ and B6$^{tg/tg}$ CMCs, the approximately 50-kDa band appeared to arise from cross-recognition of an unknown protein by the SgIGSF antibody rather than its specific recognition of another form of SgIGSF.

We also examined the expression of several intercellular adhesion molecules in CMCs with mutant MITFs. Expression levels of E-cadherin, N-cadherin, ICAM-1, and integrin β3 in B6$^{mi/mi}$, B6$^{tg/tg}$, and B6-*Mi^{wh}/Mi^{wh}* CMCs were comparable with those of B6$^{+/+}$ CMCs (Figure 1B).

CMCs were obtained from WB$^{+/+}$, WB$^{W/W}$, WBB6F$_1$$^{+/+}$, and WBB6F$_1$$^{W/W^v}$ mice, and the expression of KIT and SgIGSF was examined using anti-KIT and anti-SgIGSF antibodies. KIT signals were detected in the lysates of B6$^{+/+}$, WB$^{+/+}$, and WBB6F$_1$$^{+/+}$ CMCs, whereas no specific signals were found in the lysate of WB$^{W/W}$ CMCs (Figure 2). In WBB6F$_1$-*W/W^v* CMCs, KIT signals were detectable at significantly reduced levels (Figure 2). Next, the blot was reacted with the anti-SgIGSF antibody. WBB6F$_1$$^{W/W^v}$ CMCs expressed SgIGSF as abundantly as WBB6F$_1$$^{+/+}$ CMCs, and WB$^{W/W}$ CMCs expressed a rather higher level of SgIGSF than did WB$^{+/+}$ CMCs (Figure 2). In the lysates of CMCs from WB and WBB6F$_1$ mice, the band of approximately 50 kDa was recognized much more strongly by the SgIGSF antibody than in the lysates of CMCs from B6 mice.

Tissue distribution of SgIGSF

We examined the expression of SgIGSF in various tissues of B6$^{tg/tg}$ mice. Lysates of testes, spleens, lungs, and stomachs were obtained from B6$^{+/+}$ and B6$^{tg/tg}$ mice and were blotted with the anti-SgIGSF antibody. In spite of the remarkable difference in SgIGSF expression between B6$^{+/+}$ and B6$^{tg/tg}$ CMCs, the expression was comparable between testis, lung, spleen, and stomach tissues of B6$^{+/+}$ and B6$^{tg/tg}$ mice (Figure 3A). When the lysate of +/+ CMCs was treated with PNGase F, the mobility size of the approximately 110-kDa SgIGSF decreased to approximately 70 kDa, indicating heavy *N*-glycosylation (Figure 3B). On the other hand, the approximately 38-kDa form was not influenced by the PNGase F treatment. Similar results were obtained when the lysate of B6$^{+/+}$ testes were treated with PNGase F (Figure 3B). The variability of the molecular weights of SgIGSF observed in CMCs, NIH/3T3 transfectants, and tissues seemed to reflect the presence of various forms of SgIGSF that have received cell and tissue type-specific glycosylation.

Localization of SgIGSF

CMCs of various genotypes were cultured in suspension in the presence of PWM-SCM. Cytospin preparations of the suspension-cultured CMCs were made and stained with anti-SgIGSF antibody. When aggregates of B6$^{+/+}$ CMCs were observed, the SgIGSF-specific fluorescence was detected in the area of cell-to-cell contact (Figure 4A). The SgIGSF-specific fluorescence was not detectable in B6$^{+/+}$ CMCs that were isolated from each other. Even when aggregates of B6$^{tg/tg}$ CMCs were observed in cytospin preparations, no SgIGSF-specific fluorescence was detectable (Figure 4B). No SgIGSF-specific fluorescence was observed in aggregated B6$^{mi/mi}$ CMCs, either (data not shown). We also examined the localization of SgIGSF in the coculture of CMCs and NIH/3T3 fibroblasts. CMCs of various genotypes were plated onto the monolayer of NIH/3T3 cells that had attached to a cover slip. After 3 hours' coculture, the peripheral margin of B6$^{+/+}$ CMCs adhering to NIH/3T3 cells was clearly demarcated with the anti-SgIGSF antibody (Figure 4C). The peripheral margin of neither B6$^{tg/tg}$ nor B6$^{mi/mi}$ CMCs cocultured with NIH/3T3 cells was demarcated with the anti-SgIGSF antibody (data not shown). A sectional view of the coculture revealed that SgIGSF-specific fluorescence was concentrated on the lateral membrane of CMCs that faced the NIH/3T3 cells (Figure 4C). When the polymerized actin filaments in the coculture of B6$^{+/+}$ CMCs and NIH/3T3 cells were visualized with phalloidin, densely stained actin filaments were detected in the peripheral margins of adhering B6$^{+/+}$ CMCs. These stains colocalized with SgIGSF (Figure 4D-F). This indicated the localization of SgIGSF in lamellipodial structure. The immunocytochemical finding that NIH/3T3 cells were not stained with the anti-SgIGSF antibody was consistent with the result of Western blot analysis (Figures 1C and 4C).

Transfection of cDNAs encoding SgIGSF or +-MITF

Spleen cells of B6$^{tg/tg}$ and B6$^{mi/mi}$ mice were cocultured with Ψ2 packaging cells transformed with the retrovirus vector containing the SgIGSF cDNA. As a control, B6$^{tg/tg}$ spleen cells were cocultured with the packaging cells transformed with either the retrovirus vector containing the +-MITF cDNA or the empty vector. All 4 types of cocultures were maintained in the presence of PWM-SCM and the selective drug. Four weeks after initiation of the coculture,

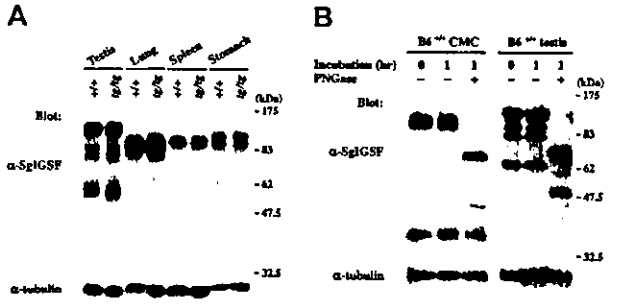

Figure 3. SgIGSF expression in various tissues of B6 $^{tg/tg}$ mice. (A) Expression of the SgIGSF protein in testis, lung, spleen, and stomach tissues of B6$^{+/+}$ and B6$^{tg/tg}$ mice. Lysates were prepared from the indicated tissues and were blotted with the anti-SgIGSF antibody. (B) *N*-linked glycosylation of SgIGSF proteins in B6$^{+/+}$ CMCs and testes. Lysates of B6$^{+/+}$ CMCs and testes were incubated at 37°C for 1 hour in the presence (+) or absence (−) of PNGase F and blotted with the anti-SgIGSF antibody. The molecular weight scale is shown to the right of the blots. The blots were probed again with the anti–α-tubulin antibody to indicate the total amount of proteins loaded per lane.

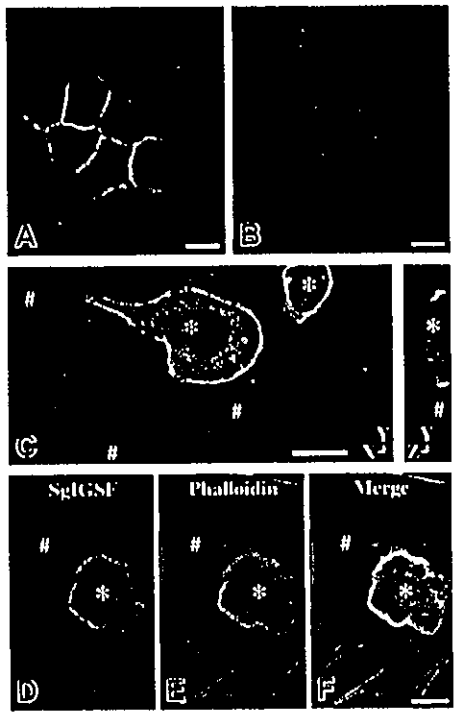

Figure 4. Immunolocalization of SgIGSF in CMCs. Immunocytochemical analysis of $B6^{+/+}$ (A) and $B6^{tg/tg}$ (B) CMCs. Cytospin preparations of CMCs were fixed with methanol, reacted with the anti-SgIGSF antibody, and stained with FITC-labeled secondary antibody. Bar, 10 μm. (C) Immunocytochemical analysis of the coculture of $B6^{+/+}$ CMCs and NIH/3T3 cells. CMCs were cocultured on the monolayer of NIH/3T3 cells for 3 hours. The coculture was fixed with methanol, reacted with the anti-SgIGSF antibody, and stained with FITC-labeled antibody. A representative set of X-Y and Y-Z sections is shown. A red line indicates the plane of the Y-Z section. (D-F) Colocalization of SgIGSF with polymerized actin filaments in the peripheral margin of $B6^{+/+}$ CMCs that have adhered to NIH/3T3 cells. After CMCs were cocultured on the monolayer of NIH/3T3 cells for 3 hours, the coculture was fixed with paraformaldehyde, reacted with the anti-SgIGSF antibody, and stained with FITC-labeled secondary antibody (D). Subsequently, the culture was stained with TRITC-labeled phalloidin (E) and the FITC and TRITC images were merged (F). *$B6^{+/+}$ CMCs; #NIH/3T3 cells. Bars, 10 μm.

Figure 5. Expression of the SgIGSF protein in $B6^{tg/tg}$ and $B6^{mi/mi}$ CMCs transfected with SgIGSF cDNA. $B6^{tg/tg}$ CMCs were infected with the empty retroviral vector (*tg/tg* CMC^{Vector}) or the vector containing either SgIGSF cDNA (*tg/tg* CMC^{SgIGSF}) or +-MITF cDNA (*tg/tg* $CMC^{MITF+/-}$). $B6^{mi/mi}$ CMCs were infected with the vector containing the SgIGSF cDNA (*mi/mi* CMC^{SgIGSF}). Lysates of the indicated cells were electrophoresed and blotted with the anti-SgIGSF and anti-MITF antibodies. After stripping, the blot was probed with the anti–α-tubulin antibody to indicate the total amount of proteins loaded per lane.

more than 95% of the floating cells were CMCs in all 4 types of coculture. Thus, coculture with the packaging cells did not influence the purity of CMCs. Obtained CMCs were examined for their expression levels of SgIGSF by Western blot. Prominent expression of SgIGSF was detected in the lysates of $B6^{tg/tg}$ and $B6^{mi/mi}$ CMCs transfected with SgIGSF cDNA (Figure 5). When the band intensity was normalized with the immunoreactivity to the antitubulin antibody, the expression levels of SgIGSF in $B6^{tg/tg}$ and $B6^{mi/mi}$ CMCs transfected with SgIGSF cDNA were more than 10-fold higher than the level of $B6^{+/+}$ CMCs. When the protein samples were loaded equally per lane, the approximately 50-kDa band was detected in the lysates of $B6^{tg/tg}$ and $B6^{mi/mi}$ CMCs transfected with SgIGSF cDNA as strongly as in the lysates of $B6^{tg/tg}$ and $B6^{mi/mi}$ CMCs (data not shown). The expression level of SgIGSF in $B6^{tg/tg}$ CMCs transfected with +-MITF cDNA was comparable with that of $B6^{+/+}$ CMCs (Figure 5). The blot was probed again with the anti-MITF antibody. Although the expression level of the endogenous +-MITF in $B6^{+/+}$ CMCs was below the limit of detection, the expression of +-MITF was detectable in $B6^{tg/tg}$ CMCs transfected with +-MITF cDNA (Figure 5). Neither SgIGSF nor MITF expression was observed in the original $B6^{tg/tg}$ CMCs or those transfected with the empty vector (Figure 5). $B6^{tg/tg}$ CMCs transfected with SgIGSF cDNA started forming macroscopic aggregates beginning 4 weeks after culture of $B6^{tg/tg}$ spleen cells was initiated (Figure 6A-B). Similar aggregates were formed by $B6^{mi/mi}$ CMCs transfected with SgIGSF cDNA (data not shown). On the other hand, $B6^{tg/tg}$ CMCs transfected with +-MITF cDNA did not form such aggregates (data not shown). The appearance of $B6^{tg/tg}$ CMCs transfected with +-MITF was similar to the appearance of $B6^{+/+}$ CMCs.

In the culture of $B6^{tg/tg}$ and $B6^{mi/mi}$ CMCs transfected with SgIGSF cDNA, both the number of aggregates and the number of cells in each aggregate continually increased after the fourth week of culture. In the fifth week of culture, the number of cells forming aggregates reached more than half the number of total cells in each culture, and some aggregates contained more than 100 cells. The aggregated CMCs did not appear to grow as fast as intact $B6^{tg/tg}$ and

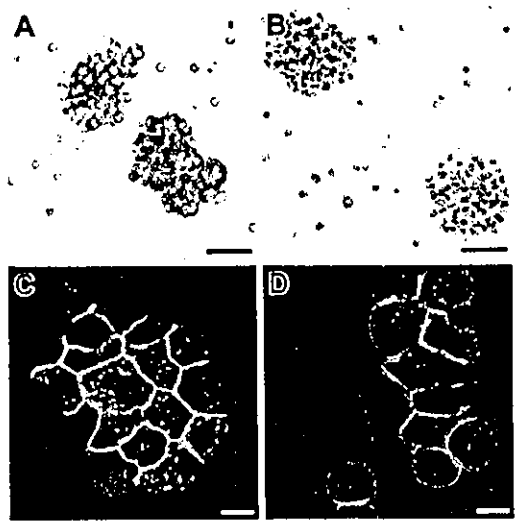

Figure 6. Phenotypes of $B6^{tg/tg}$ CMCs transfected with SgIGSF or +-MITF. (A) Phase contrast image of $B6^{tg/tg}$ CMCs transfected with SgIGSF cDNA. Aggregates of the CMCs were floating in the medium. Bar, 50 μm. (B) Aggregates composed of numerous alcian blue–positive cells. Cytospin samples of $B6^{tg/tg}$ CMCs transfected with SgIGSF cDNA were stained with alcian blue and nuclear fast red. Bar, 50 μm. (C,D) Immunocytochemical analysis of $B6^{tg/tg}$ CMCs transfected with either SgIGSF cDNA (C) or +-MITF cDNA (D). Cytospin preparations of either type of cells were fixed with methanol, reacted with the anti-SgIGSF antibody, and stained with FITC-labeled secondary antibody. Bar, 10 μm.